(Fig. 1g). Finally, TDP-43 immunoreactivity tended to be more intense in anterior part of the hippocampus and parahippocampal gyrus than in posterior part of those in most cases. This pathological distribution was again in accordance with an AGs staging system that reflects an antero-posterior gradient in the putative progression of AGD [7, 24].

Colocalization of TDP-43 immunoreactive structures and tau positive structures

Double-labeling confocal microscopy revealed virtually no colocalization of phospho-tau and phospho-TDP-43 in the dentate gyrus of the hippocampus (Fig. 2a–c). In the entorhinal cortex and the amygdala, however, occasional colocalization of phospho-tau and phospho-TDP-43 was observed in the neuronal cytoplasmic inclusions and grain-like structures in neuropil (Fig. 2d–f). In neurons that showed cytoplasmic co-existence of both proteins, phospho-TDP-43 positive structures were sometimes separated from phospho-tau (Fig. 2g, h).

Confirmation of TDP-43 immunoreactivity through various methods

The staining patterns obtained with pS409/410, a phosphorylation-specific antibody (Fig. 1d–i), were almost same as those obtained with pS403/404, another phosphorylation-specific antibody (Fig. 3b, f). They stained only abnormal structures with no nuclear staining. Anti-TDP43C (405–414), a phosphorylation-independent C-terminal antibody, showed similar staining to those except for a weak staining of normal nuclei (Fig. 3c). Commercial antibody (10782-2-AP) and anti-TDP43N [3–12], a phosphorylation-independent N-terminal antibody, also stained abnormal structures with intense nuclear staining (Fig. 3a, d, e). Because of such nuclear staining, it was difficult to identify grain-like structures using these phosphorylation-independent antibodies.

In four cases for which both formalin-fixed paraffin-embedded sections and 4% PFA-fixed free-floating frozen sections were available, one case showed TDP-43 immunoreactivity. In this case, however, a significant difference of

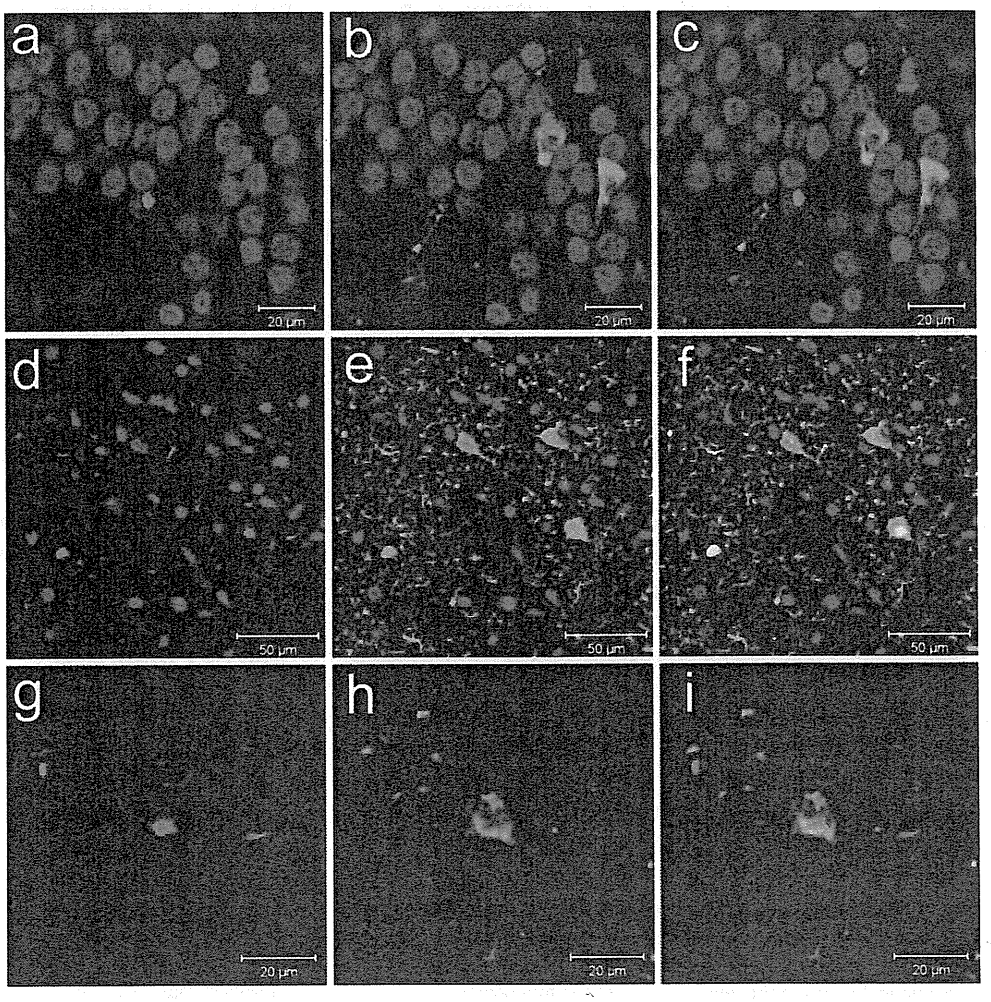

Fig. 2 Confocal double-immunofluorescence of phospho-TDP43 (**a**, **d**, **g**) and phospho-tau (**b**, **e**, **h**). Merged images are shown in **c**, **f** and **i**. In the granular cells in the dentate gyrus of the hippocampus, a TDP-43 positive neuronal cytoplasmic inclusion (*red* fluorescence in **a** and **c**) is not colocalized with tau labeling (*green* fluorescence in **b** and **c**). In the entorhinal cortex, small dot-like structures, short dystrophic neurites and round inclusions are immunopositive for TDP-43 (**d**), and a lot of grains and neurons are positive for tau (**e**). Partial colocalization is seen in some grain-like structures in the neuropil and neuronal cytoplasmic inclusions (*yellow* in **f**). Nuclei are stained with TO-PRO-3 (Invitrogen, Tokyo, Japan), producing a blue color. A higher magnification of co-existence of phospho-tau and phospho-TDP-43 seen in the same neurons (**g–i**). Most of phospho-TDP-43 positive structure (*red* in **g** and **h**) is separated from phospho-tau (*green* in **h** and **i**)

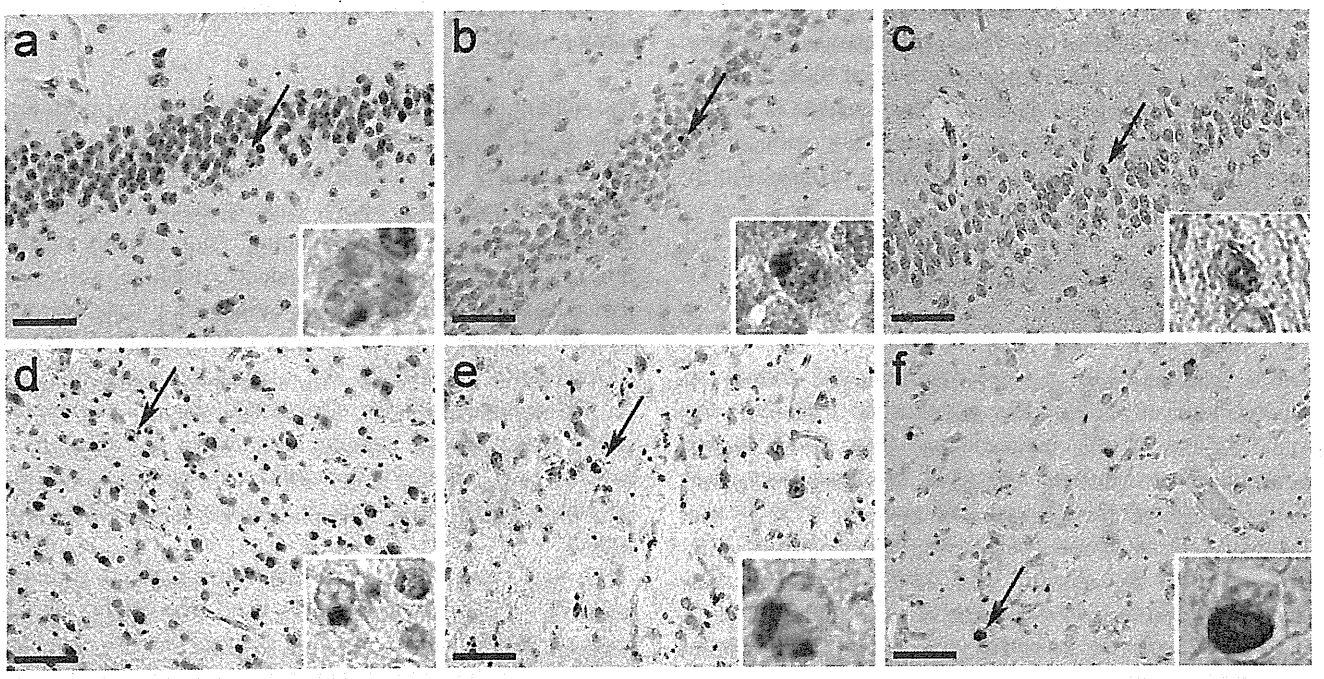

Fig. 3 Immunohistochemistry using a panel of anti-TDP-43 antibodies. Immunostaining of dentate gyrus of the hippocampus (**a–c**) and amygdala (**d–f**) using commercial phosphorylation-independent antibody (10782-2-AP, Protein Tech) (**a**, **d**), pS403/404 (**b**, **f**), anti-TDP43C (405–414) (**c**), and anti-TDP43N [3–12] (**e**). All antibodies positively stain neuronal cytoplasmic inclusions. Note that it is easier to recognize neuronal cytoplasmic inclusions by pS403/404 (**b**, **f**) and anti-TDP43C (405–414) (**c**) than by a commercial antibody to TDP-43 (**a**, **d**) and anti-TDP43 N [3–12] (**e**), which intensely stain normal nuclei. Each inset in a lower right corner represents a higher magnification of the region indicated by an *arrow* (*bars* 50 μm)

the immunoreactivity was observed between the sections. In free-floating sections, massive TDP-43 positive grain-like structures in the neuropil in the entorhinal cortex (Fig. 4a) and neuronal cytoplasmic inclusions in the dentate fascia (Fig. 4b) were recognized, while in paraffin-embedded sections, only occasional neuronal cytoplasmic inclusions were seen in CA1 of the hippocampus. This discrepancy of immunoreactivity may be due to methodological differences including a fixation and a treatment of brain tissues.

Relationship of TDP-43 immunoreactivity to demographics and pathological variables

There were no differences in age at death, disease duration, sex, brain weight, NFT Braak stage, or severity of amyloid burden between AGD cases with and without TDP-43 immunoreactivity. Clinical diagnoses are varied in both AGD cases with and without TDP-43 immunoreactivity: four senile dementia, one Alzheimer's disease, one vascular dementia, one Parkinson's disease with dementia, two schizophrenia in nine AGD cases with TDP-43 immunoreactivity, and one senile dementia, one alcoholic dementia, one dementia with Lewy bodies, one senile psychosis, one unclassified dementia, one schizophrenia in six AGD cases without TDP-43 immunoreactivity. There was no AGD case with clinical diagnosis of FTLD in this series. AGD cases with TDP-43-immunoreactivity had higher AGD stages than those without TDP-43 immunoreactivity ($P < 0.05$). The frequency of TDP-43 immunoreactivity was correlated with AGD stage ($r = 0.62$, $P = 0.01$), and with CERAD plaque scores ($r = -0.53$, $P = 0.03$), but not with NFT Braak stage ($r = 0.06$, $P = 0.80$).

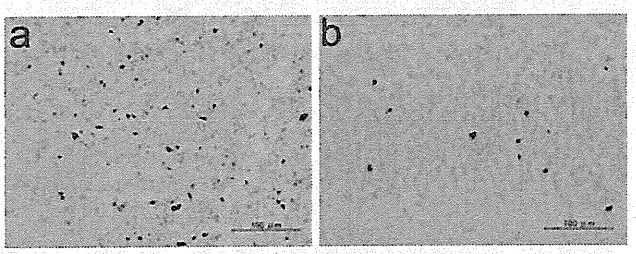

Fig. 4 Immunohistochemistry of free-floating sections of case #3 using pS409/410. **a** Massive grain-like or dot-like structures and short dystrophic neurites in the entorhinal cortex. **b** A lot of neuronal cytoplasmic inclusions in the dentate gyrus of the hippocampus

Discussion

By immunohistochemical examinations using a panel of phosphorylation-dependent and -independent antibodies to TDP-43, in this study, we demonstrated a high frequency (60%) of TDP-43 pathology in AGD cases for the first time. The limbic regions, especially the amygdala and the anterior part of the parahippocampal gyrus, showed the

Table 3 Comparison of AGD with and without TDP43-immunoreactive pathology

	TDP-43 positive ($N = 9$)	TDP-43 negative ($N = 6$)	P value
Age at death ± SD (years)	82.8 ± 6.7	85.8 ± 8.9	NS
Disease duration ± SD, (years)	5.5 ± 3.0 ($N = 6$)	7.2 ± 3.4 ($N = 4$)	NS
Sex ratio (F/M)	4/5	3/3	NS
Brain weight ± SD (gm)	1124 ± 102	1121 ± 155	NS
NFT Braak stage (25th, 75th percentile)	2.0(1.25, 2.0)	2.0 (1.0, 2.75)	NS
CERAD plaque score (25th, 75th percentile)	2.0 (0.0, 2.0)	2.5 (2.0, 3.0)	NS
AGD stage (25th, 75th percentile)	2.0 (1.75, 3.0)	1.0 (1.0, 1.0)	$P < 0.05$

There was no difference in demographics between cases with and without TDP-43 immunoreactivity. AGD cases with TDP-43 immunoreactivity had higher AGD stages than those without TDP-43 immunoreactivity ($P < 0.05$), but there was no difference in NFT Braak stages and CERAD plaque scores between them

NS not significant, *NFT* neurofibrillary tangle, *CERAD* Consortium to Establish a Registry for Alzheimer Disease Guidelines, *AGD* argyrophilic grain disease

most frequent and severe TDP-43 pathology. These findings are consistent with the previous reports of TDP-43 pathology in AD and LBD [13, 14].

Recent reports have revealed various degrees of co-occurrence of TDP-43 immunoreactivity in a variety of neurodegenerative disorders, including AD, LBD, CBD, Guamanian ALS/PDC and Huntington's disease [1, 9, 11, 13, 21, 25, 30]. Amador–Ortiz reported that 20–30% of AD and 70% of hippocampal sclerosis had TDP-43 immunoreactivity [1]. All AGD cases employed in this study did not fulfill the pathological criteria of AD, and there is no significant difference of Braak staging between cases with TDP-43 immunoreactivity and those without TDP-43 immunoreactivity (Table 3). Although only one AGD case with hippocampal sclerosis was included in our series, that case showed no TDP-43 immunoreactivity. Thus, it is unlikely that a high frequency of TDP-43 pathology in this AGD series is due to concurrent AD or hippocampal sclerosis.

In this AGD series, although the concomitant TDP-43 pathology was the most severe in the limbic structures, many cases showed the extension of TDP-43 pathology into the temporal neocortices. It is currently unknown if this represents concurrent primary pathological process of FTLD-U, or a secondary change occurring in susceptible neuronal populations. At least, a simple coincidence of FTLD-U and AGD seems unlikely based on our findings as follows. First, the frequency of TDP-43 positive neuronal cytoplasmic inclusions in the dentate gyrus, which are one of the pathological hallmarks of FTLD-U, is low (22%) in our AGD cases with TDP-43 immunoreactivity. Second, TDP-43 positive grain-like structures found in our AGD cases have not been reported in FTLD-U brains so far. Third, parallel distribution of TDP-43 positive structures and tau positive AGs and a higher AGD stages in cases with TDP-43 immunoreactivity than in those without TDP-43 immunoreactivity suggest some relationships between accumulation of TDP-43 and that of tau. Double label immunofluorescence microscopy revealed partial colocalization of phospho-tau and phospho-TDP-43 in grain-like structures and neuronal cytoplasmic inclusions in this study. Such partial colocalization of tau and TDP-43 is consistent with that previously reported in AD, LBD, Guamanian PDC and CBD [1, 2, 8, 11, 13, 21]. Although these findings may not suggest a direct interaction between tau and TDP-43, there may be common factors or mechanisms that affect the conformation or modification of both proteins, leading to their intracellular accumulation.

Ikeda et al. [15] reported that the clinical features of AGD consist of personality changes characterized by emotional disorder with aggression or ill temper and relatively preserved cognitive function. These clinical features are also observed in FTLD. In this study, however, none of AGD cases, including the case with massive TDP-43 pathology (Fig. 4), had a clinical diagnosis of FTLD. Moreover, there was no significant difference in demographics, including age at death, disease duration, sex and brain weight, between AGD cases with TDP-43 pathology and those without TDP-43 pathology. These findings suggest the possibility that TDP-43 pathology does not have a significant impact on the clinical presentation of AGD. This is consistent with the previous report by Uryu et al. [30] that showed a lack of association between TDP-43 pathology and clinical manifestations in AD. It should be noted, however, that in the present study, a sample size was small and only a limited set of clinical manifestations was examined. Further studies using more detailed associations with larger data sets on behavioral impairments in AGD should be performed.

Acknowledgments The assistance of Kyoko Suzuki, Chie Haga and Hiromi Kondo for histologic and immunohistochemistry studies is greatly appreciated. We are grateful to Dr. de Silva for generous supply of RD4 antibody.

References

1. Amador-Ortiz C, Lin WL, Ahmed Z et al (2007) TDP-43 immunoreactivity in hippocampal sclerosis and Alzheimer's disease. Ann Neurol 61:435–445
2. Arai T, Hasegawa M, Akiyama H et al (2006) TDP-43 is a component of ubiquitin-positive tau-negative inclusions in frontotemporal lobar degeneration and amyotrophic lateral sclerosis. Biochem Biophys Res Commun 351:602–611
3. Braak H, Braak E (1987) Argyrophilic grains: characteristic pathology of cerebral cortex in cases of adult onset dementia without Alzheimer changes. Neurosci Lett 76:124–127
4. Braak H, Braak E (1989) Cortical and subcortical argyrophilic grains characterize a disease associated with adult onset dementia. Neuropathol Appl Neurobiol 15:13–26
5. Braak H, Braak E (1991) Neuropathological stageing of Alzheimer-related changes. Acta Neuropathol 82:239–259
6. Cairns NJ, Neumann M, Bigio EH et al (2007) TDP-43 in familial and sporadic frontotemporal lobar degeneration with ubiquitin inclusions. Am J Pathol 171:227–240
7. Ferrer I, Santpere G, van Leeuwen FW (2008) Argyrophilic grain disease. Brain 131:1416–1432
8. Freeman SH, Spires-Jones T, Hyman BT, Growdon JH, Frosch MP (2008) TAR-DNA binding protein 43 in Pick disease. J Neuropathol Exp Neurol 67:62–67
9. Geser F, Winton MJ, Kwong LK et al (2008) Pathological TDP-43 in parkinsonism-dementia complex and amyotrophic lateral sclerosis of Guam. Acta Neuropathol 115:133–145
10. Gitcho MA, Baloh RH, Chakraverty S et al (2008) TDP-43 A315T mutation in familial motor neuron disease. Ann Neurol. doi:10.1002/ana.21344
11. Hasegawa M, Arai T, Akiyama H et al (2007) TDP-43 is deposited in the Guam parkinsonism-dementia complex brains. Brain 130:1386–1394
12. Hasegawa M, Arai T, Nonaka T et al (2008) Phosphorylated TDP-43 in frontotemporal lobar degeneration and amyotrophic lateral sclerosis. Ann Neurol 64:60–70
13. Higashi S, Iseki E, Yamamoto R et al (2007) Concurrence of TDP-43, tau and alpha-synuclein pathology in brains of Alzheimer's disease and dementia with Lewy bodies. Brain Res 1184:284–294
14. Hu WT, Josephs KA, Knopman DS et al (2008) Temporal lobar predominance of TDP-43 neuronal cytoplasmic inclusions in Alzheimer disease. Acta Neuropathol 116:215–220
15. Ikeda K, Akiyama H, Arai T et al (2000) Clinical aspects of argyrophilic grain disease. Clin Neuropathol 19:278–284
16. Inukai Y, Nonaka T, Arai T et al (2008) Abnormal phosphorylation of Ser409/410 of TDP-43 in FTLD-U and ALS. FEBS Lett 582:2899–2904
17. Ishizawa T, Ko LW, Cookson N, Davias P, Espinoza M, Dickson DW (2002) Selective neurofibrillary degeneration of the hippocampal CA2 sector is associated with four-repeat tauopathies. J Neuropathol Exp Neurol 61:1040–1047
18. Kabashi E, Valdmanis PN, Dion P et al (2008) TARDBP mutations in individuals with sporadic and familial amyotrophic lateral sclerosis. Nat Genet 40:572–574
19. Mackenzie IR, Bigio EH, Ince PG et al (2007) Pathological TDP-43 distinguishes sporadic amyotrophic lateral sclerosis from amyotrophic lateral sclerosis with SOD1 mutations. Ann Neurol 61:427–434
20. Mirra SS, Heyman A, McKeel D et al (1991) The Consortium to Establish a Registry for Alzheimer's Disease (CERAD). Part II. Standardization of the neuropathologic assessment of Alzheimer's disease. Neurology 41:479–486
21. Nakashima-Yasuda H, Uryu K, Robinson J et al (2007) Co-morbidity of TDP-43 proteinopathy in Lewy body related diseases. Acta Neuropathol 114:221–229
22. Neumann M, Sampathu DM, Kwong LK et al (2006) Ubiquitinated TDP-43 in frontotemporal lobar degeneration and amyotrophic lateral sclerosis. Science 314:130–133
23. Neumann M, Mackenzie IR, Cairns NJ et al (2007) TDP-43 in the ubiquitin pathology of frontotemporal dementia with VCP gene mutations. J Neuropathol Exp Neurol 66:152–157
24. Saito Y, Ruberu NN, Sawabe M et al (2004) Staging of argyrophilic grains: an age-associated tauopathy. J Neuropathol Exp Neurol 63:911–918
25. Schwab C, Arai T, Hasegawa M, Yu S, McGeer PL (2008) Colocalization of TDP-43 and huntingtin in inclusions of Huntington's disease. J Neuropathol Exp Neurol (in press)
26. Sreedharan J, Blair IP, Tripathi VB et al (2008) TDP-43 mutations in familial and sporadic amyotrophic lateral sclerosis. Science 319:1668–1672
27. Tan CF, Eguchi H, Tagawa A et al (2007) TDP-43 immunoreactivity in neuronal inclusions in familial amyotrophic lateral sclerosis with or without SOD1 gene mutation. Acta Neuropathol 113:535–542
28. Togo T, Sahara N, Yen SH et al (2002) Argyrophilic grain disease is a sporadic 4-repeat tauopathy. J Neuropathol Exp Neurol 61:547–556
29. Togo T, Cookson N, Dickson DW (2002) Argyrophilic grain disease: neuropathology, frequency in a dementia brain bank and lack of relationship with apolipoprotein E. Brain Pathol 12:45–52
30. Uryu K, Nakashima-Yasuda H, Forman MS et al (2008) Concomitant TAR-DNA-binding protein 43 pathology is present in Alzheimer disease and corticobasal degeneration but not in other tauopathies. J Neuropathol Exp Neurol 67:555–564
31. Van Deerlin VM, Leverenz JB, Bekris LM et al (2008) TARDBP mutations in amyotrophic lateral sclerosis with TDP-43 neuropathology: a genetic and histopathological analysis. Lancet Neurol 7:409–416
32. Yokoseki A, Shiga A, Tan CF et al (2008) TDP-43 mutation in familial amyotrophic lateral sclerosis. Ann Neurol 63:538–542

Biochemical and Biophysical Research Communications 382 (2009) 405–409

Contents lists available at ScienceDirect

Biochemical and Biophysical Research Communications

journal homepage: www.elsevier.com/locate/ybbrc

Identification of casein kinase-1 phosphorylation sites on TDP-43

Fuyuki Kametani [a,*], Takashi Nonaka [a], Takehiro Suzuki [c], Tetsuaki Arai [b], Naoshi Dohmae [c], Haruhiko Akiyama [b], Masato Hasegawa [a]

[a] Department of Molecular Neurobiology, Tokyo Institute of Psychiatry, Tokyo Metropolitan Organization for Medical Research, Kamikitazawa 2-1-8, Setagaya-ku, Tokyo 156-8585, Japan
[b] Department of Psychogeriatrics, Tokyo Institute of Psychiatry, Tokyo Metropolitan Organization for Medical Research, Tokyo 156-8585, Japan
[c] Biomolecular Characterization Team, Advanced Development and Supporting Center, The Institute of Physical and Chemical Research (RIKEN), Hirosawa 2-1, Wako, Saitama 351-0198, Japan

ARTICLE INFO

Article history:
Received 5 March 2009
Available online 13 March 2009

Keywords:
TDP-43
Phosphorylation
Casein kinase-1
Frontotemporal lobar degeneration with ubiquitin-positive inclusions
Amyotrophic lateral sclerosis
Mass spectrometry

ABSTRACT

TAR DNA-binding protein of 43 kDa (TDP-43) is deposited as hyperphosphorylated cytoplasmic and intranuclear inclusions in brains of patients with frontotemporal lobar degeneration with ubiquitinated inclusions and amyotrophic lateral sclerosis. In this study, we identified 29 phosphorylation sites on recombinant TDP-43 that are phosphorylated by casein kinase-1 (CK1). Interestingly, 18 of them were located in the C-terminal glycine-rich region of TDP-43. Our results indicate that CK1-mediated phosphorylation may play a role in the pathogenesis of these diseases.

Introduction

TAR DNA-binding protein 43 (TDP-43), encoded by the *TARDBP* gene on chromosome 1, is a highly conserved, ubiquitously expressed nuclear protein. It regulates gene transcription, exon splicing, and exon inclusion [1–4], and is also a multifunctional RNA-binding protein [4]. Recently, TDP-43 was identified as a major disease-associated protein in frontotemporal lobar degeneration with ubiquitin-positive inclusions (FTLD-U) and in amyotrophic lateral sclerosis (ALS) [5,6]. We previously reported that deposited TDP-43 is abnormally phosphorylated, and several antibodies raised against synthetic phosphorylated TDP-43 peptides recognized the pathological structures in FTLD-U and ALS [7]. Immunoblot analysis with these antibodies showed that the Sarkosyl-insoluble fraction extracted from brains of patients with FTLD-U and ALS contains hyperphosphorylated TDP-43 with a molecular weight of 45 kDa, together with fragments of 18–28 kDa [7,8]. Similar characteristic band patterns were obtained in the case of cultured cells expressing mutant TDP-43 [9]. In an in vitro phosphorylation assay of recombinant TDP-43, the product(s) of casein kinase-1 (CK1) phosphorylation showed similar electrophoretic mobility to that of hyperphosphorylated TDP-43 present in the brains of patients with FTLD-U and ALS, suggesting that CK1 may be involved in the hyperphosphorylation of TDP-43 [7,8]. To date, however, there is little information about the sites of the putative CK1-mediated hyperphosphorylation on TDP-43. In this study, we identified multiple sites on recombinant TDP-43 that are phosphorylated by CK1; in particular, the C-terminal Gly-rich region of TDP-43 appears to have a favorable conformation for CK1-mediated phosphorylation.

Materials and methods

TDP-43 construct and in vitro phosphorylation of TDP-43. Human TDP-43 cDNA was subcloned into pRK172 expression vectors and transformed into *Escherichia coli* BL21 (DE3) [7]. Crude extracts from *E. coli* expressing human TDP-43 were applied to a heparin-Toyopearl column. The column was washed, and TDP-43 was eluted with 0.5 M NaCl solution. The eluate (partially purified TDP-43) was phosphorylated with CK1 (New England Biolabs, Beverly, MA) at 30 °C for 14 h.

SDS–polyacrylamide gel electrophoresis (PAGE) and in-gel digestion. Phosphorylated TDP-43 was separated by SDS–PAGE [7]. The band of phosphorylated TDP-43 was excised and soaked in 50 mM Tris–HCl, pH 8.0 containing 50% acetonitrile for 30 min. The gel was dried in a Speed-Vac (Savant) and incubated in 50 mM Tris–HCl, pH 8.0 containing 125–250 ng of modified trypsin

* Corresponding author. Fax: +81 3 3329 8035.
E-mail address: kametani@prit.go.jp (F. Kametani).

0006-291X/$ - see front matter © 2009 Elsevier Inc. All rights reserved.
doi:10.1016/j.bbrc.2009.03.038

(Roche Diagnostics, Mannheim, Germany), chymotrypsin (Roche Diagnostics, Mannheim, Germany), or thermolysin at 37 °C for 6–20 h. The digests were extracted from the gel twice with 100 μl of 0.1% TFA containing 60% acetonitrile. These two extracts were combined, evaporated in a Speed-Vac, and stored at −80 °C until assayed.

Liquid chromatography-ion trap mass spectrometry (LC–MS/MS). The sample was resuspended in 0.1% formic acid containing 2% acetonitrile and applied to a Paradigm MS4 (Microm BioResources Inc., Auburn, CA) HPLC system fitted with HTC-PAL automatic sampler (CHROMSYS LLC, Alexandria, VA). A reverse-phase capillary column (Develosil ODS-HG5, 0.075 mm i.d. × 50 mm or 0.075 mm i.d. × 150 mm, Nomura Chemical Co., Ltd., Seto, Japan) was used at a flow rate of 200 or 300 nl/min with a 4–80% linear gradient of acetonitrile. Eluted peptides were directly detected with an ion trap mass spectrometer, LXQ (Thermo Fisher Scientific Inc.) at a spray voltage of 1.9 kV and collision energy of 35%. The mass acquisition method consisted of one full MS survey scan followed by MS/MS scan of the most abundant precursor ions from the survey scan. Dynamic exclusion for MS/MS spectra was set to 30 s. Furthermore, if neutral loss of 98, 49, or 32.7 Da was detected (corresponding to loss of phosphoric acid from singly, doubly, and triply charged precursor ions) among the most abundant ions in the MS/MS scan, a MS/MS/MS scan was then carried out. The data were analyzed with BioWorks (Thermo Fisher Scientific Inc.) and Mascot (Matrix Science Inc., Boston, USA) software.

Calcium phosphate precipitation. Calcium phosphate precipitation was carried out as described [10]. Some extracted digests were dissolved in 44 μl of pure water, which was obtained from an EASYpure system (Barnstead International, Thermo Fisher Scientific Inc.). Then 2 μl of 0.5 M Na_2HPO_4 and 2 μl of 2 M NH_4OH were added and mixed, followed by the addition of 2 μl of 2 M $CaCl_2$. The solution was vortexed and centrifuged at 18,000*g* for 30 min. The supernatant was removed, and the precipitate was

Table 1
Identified phospho-peptides obtained from CK1 phosphorylated TDP-43.

Residue	Amino acid sequence	Charge	Mass (actual)	Mass (calculated)
Trypsin digestion				
83–95	RKMDETDASS(p)AVK	2	1516.87	1516.66
83–95	RKM(ox)DETDASS(p)AVK	2	1533.30	1532.65
84–95	KMDETDASS(p)AVK	1	1360.53	1360.65
84–95	KM(ox)DETDASS(p)AVK	2	1377.22	1376.55
85–95	MDETDASS(p)AVK	2	1233.40	1232.46
85–95	M(ox)DETDASS(p)AVK	2	1249.29	1248.46
85–95	M(ox)DETDAS(p)S(p)AVK	2	1329.16	1328.42
85–95	MDET(p)DASSAVK	2	1232.72	1232.46
85–97	MDETDASS(p)AVKVK	2	1461.46	1459.63
115–136	TT(p)EQDLKEYFSTFGEVLMVQVK	3	2688.66	2687.24
177–189	LPNSKQS(p)QDEPLR	2	1669.54	1670.71
182–189	QS(p)QDEPLR	2	1051.31	1051.43
228–251	AFAFVFTADDQIAQS(p)LCGEDLIIK	2	2694.69	2694.27
252–263	GIS(p)VHISNAEPK	2	1332.31	1330.63
269–275	QLERS(p)GR	2	925.98	924.42
276–293	FGGNPGGFGNQGGFGNS(p)R	2	1807.23	1805.73
409–414	SS(p)GWGM	1	703.22	703.20
409–414	S(p)S(p)GWGM(ox)	2	798.90	799.16
Chymotrypsin digestion				
1–27	MS(p)EY(p)IRVTEDENDEPIEIPSEDDGTVL	2	3254.58	3254.31
5–27	IRVTEDENDEPIEIPSEDDGT(p)VL	2	2664.68	2664.17
277–299	GGNPGGFGNQGGFGNS(p)RGGGAGLGNNQGSNMGGGMNF	2	2072.66	2070.87
386–401	GS(p)ASNAGSGSGFNGGF	2	1451.54	1452.53
386–401	GSAS(p)NAGSGS(p)GFNGGF	2	1533.92	1532.50
398–414	NGGFGSSMDS(p)KSSGWGM(ox)	2	1787.11	1786.63
Thermolysin digestion				
86–96	DETDASS(p)AVKV	2	1201.54	1200.49
236–249	DDQIAQS(p)LCGEDLI	2	1599.12	1598.65
242–250	S(p)LCGEDLII	1	1117.63	1117.44
270–276	LERS(p)GR	2	942.12	943.43
295–305	GGAGLGNNQGS(p)	2	1010.45	1010.38
295–308	GGAGLGNNQGS(p)NMG	2	1329.24	1328.48
301–311	NNQGS(p)NMGGGM(ox)	1	1160.60	1160.36
336–345	MMGMLAS(p)QQ	2	1189.72	1189.43
340–347	LASQQNQS(p)	2	952.61	954.38
347–354	SGPS(p)GNN	1	839.62	839.28
364–369	NQAFGS(p)	1	703.56	702.24
369–380	SGNNSYS(p)GSNS	2	1209.19	1209.39
369–380	SGNNSYSGS(p)NS(p)	2	1289.47	1289.36
385–394	WGS(p)AS(p)NAGS(p)	2	1075.07	1075.25
385–396	WGSAS(p)NAGS(p)GSG	2	1196.59	1196.35
387–397	SASNAGS(p)GSGF	2	1020.59	1020.35
391–405	AGS(p)GS(p)GFNGGFGS(p)S(p)M	2	1638.71	1638.39
393–401	SGS(p)GFNGGF	2	906.77	908.31
393–401	S(p)GSGFNGGF	2	907.44	908.31
395–405	SGFNGGFGSS(p)M	2	1126.61	1126.38
397–405	FNGGFGS(p)	2	765.47	765.25
400–410	GFGSS(p)MDSKSS	2	1185.55	1184.41
405–414	MDS(p)KS(p)S(p)GWGM(ox)	2	1340.04	1340.33

p, phosphorylation; ox, oxidation.

washed with 80 mM $CaCl_2$. After centrifugation as described above, the washing solution was removed. The pellet was dissolved in 20 μl of 5% formic acid and applied to the LXQ LC–MS/MS as described above.

Results

Recombinant TDP-43 was phosphorylated with CK1 and the products were purified by means of SDS–PAGE as described [7]. Phosphorylated TDP-43 was digested in the gel with trypsin, chymotrypsin and thermolysin. On LC–MS/MS analysis with LXQ, 18, 6, and 23 phosphorylated peptides were obtained from the trypsin, chymotrypsin, and thermolysin digests, respectively (Table 1). MS/MS analysis data for two representative peptides are shown in Fig. 1. A sequence coverage of 98% was achieved for TDP-43; residues 80–82 and 264–270 were not covered (data not shown). We identified 29 phosphorylation sites, including the previously reported Ser 91 and Ser 92 [11], as shown in Fig. 2. Interestingly, 18 of these sites were located in the C-terminal glycine-rich region (274–414) of TDP-43 (Fig. 2).

The NetPhosK 1.0 server produces neural network-based predictions of kinase-specific eukaryotic protein phosphorylation sites [12,13]. Prediction scores of CK1 phosphorylation for all serine and threonine residues in TDP-43 were calculated with this server. The scores and the actual phosphorylated sites identified as described above are summarized in Table 2. Although no significant difference of the distribution of the prediction score was seen between the 1–273 region and the 274–414 region (C-terminal Gly-rich region), CK1 clearly phosphorylated more serine/threonine residues in the 274–414 region. In particular, 12 of 14 resides in the low score range (0.36–0.39) were phosphorylated in the 274–414 region, comparing with 6 of 27 residues in the 1–273 region.

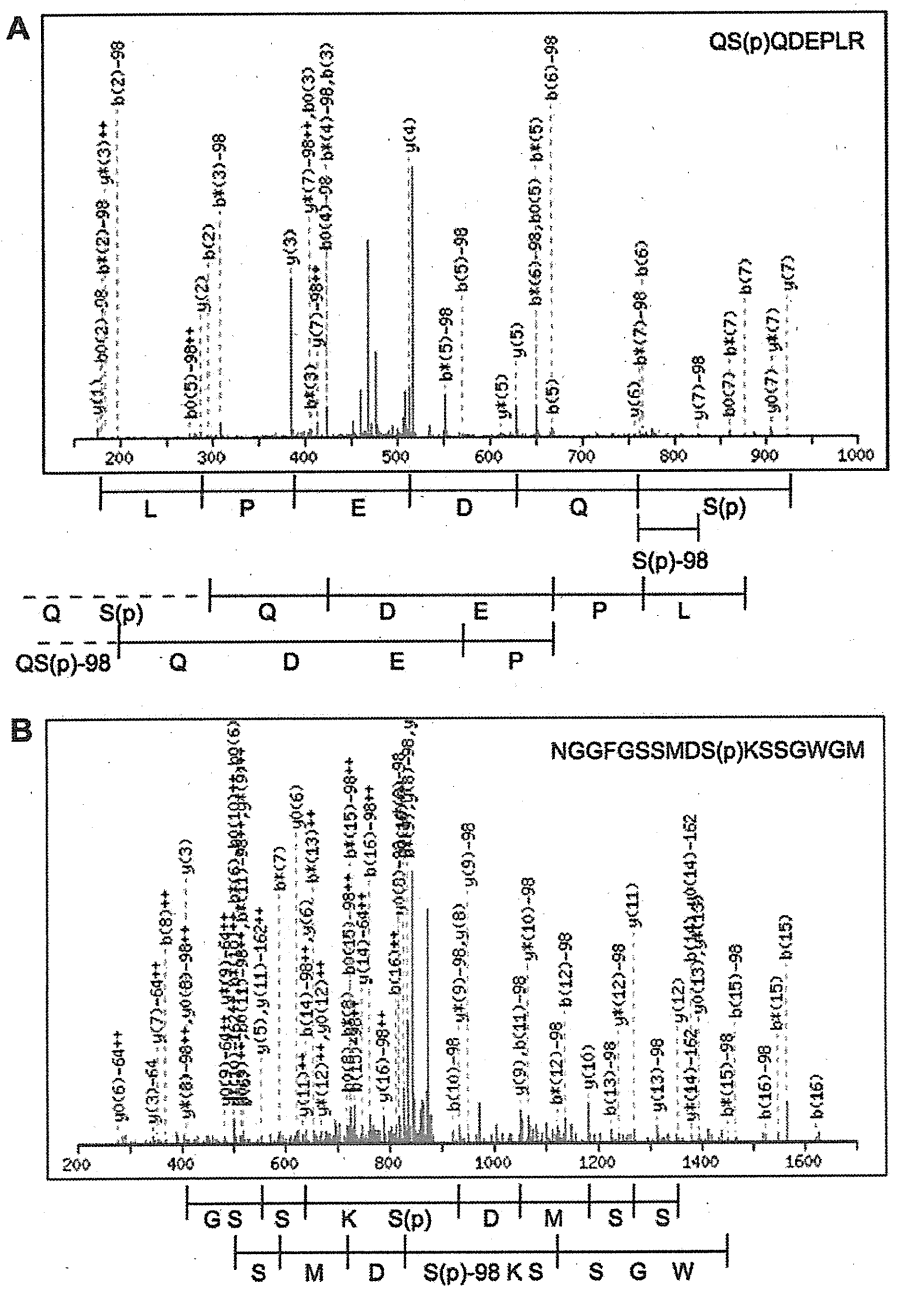

Fig. 1. Identification of phosphorylation sites by LC–MS/MS analysis. (A) Tryptic peptide, QSQDEPLR. The second Ser residue was phosphorylated. (B) Chymotryptic peptide, NGGFGGSSMDSKSSGWGM. The eleventh Ser residue was phosphorylated.

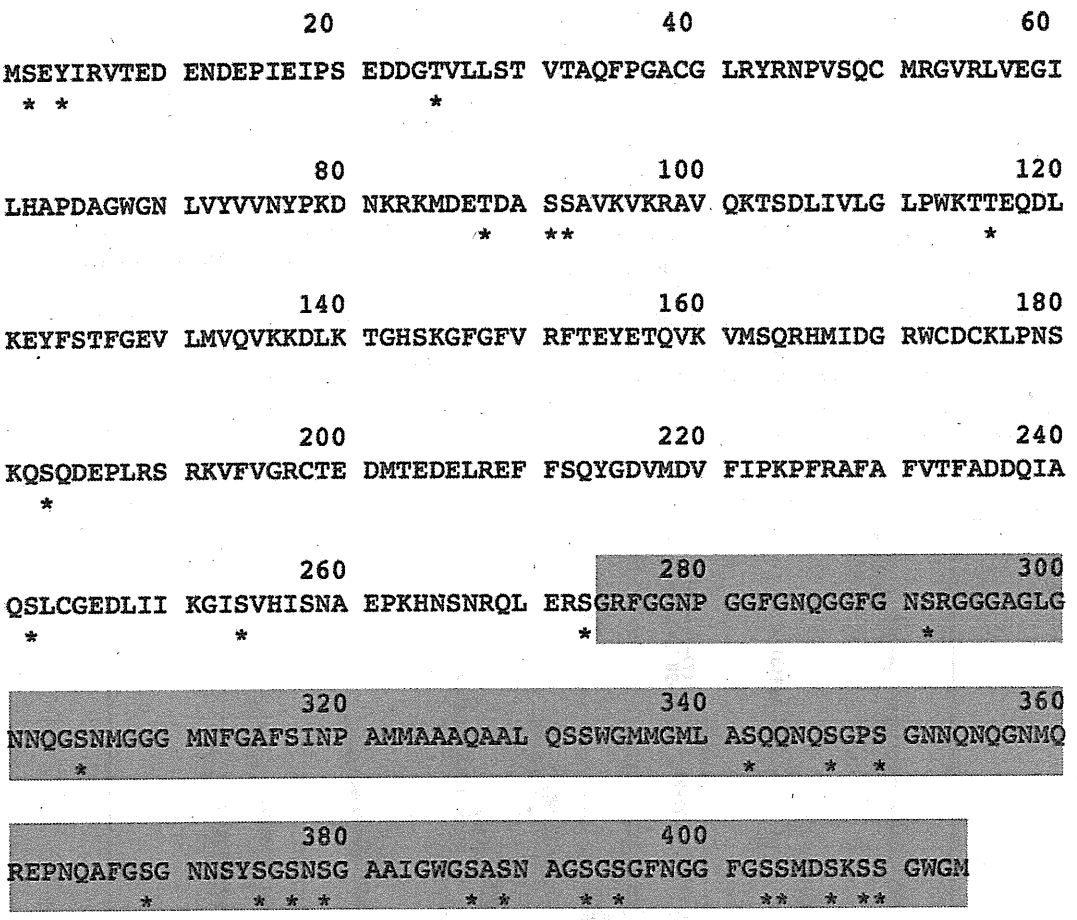

Fig. 2. CK1 phosphorylation sites on recombinant TDP-43. Asterisks show phosphorylation sites. The boxed region is the C-terminal Gly-rich region (273–414).

Table 2
The summarized table of prediction scores of CK1 phosphorylation and actual phosphorylated residues (number of phosphorylated residues/number of Ser/Thr residues).

Prediction score range	1–273	274–414 (Gly-rich region)
0.50–0.51	0	1/1
0.40–0.49	4/7	5/7
0.36–0.39	6/27	12/14

Discussion

In this experiment, we identified 29 phosphorylation sites in recombinant TDP-43, including the previously reported Ser 91 and Ser 92 [11]. In particular, 18 of them were located in the C-terminal Gly-rich region. This suggests that the C-terminal Gly-rich region has a conformation that is favorable for CK1 phosphorylation. Interestingly, among 13 pathogenic mutations (G290A, G294V, G298S, A315T, S332N, M337V, Q343R, N345K, G348C, N352S, S379P, A382T, and I383V) found in familial ALS cases and 15 variants (D169G, N267S, G287S, G294A, G295S, G295R, Q331K, G335D, G348C, R361S, S379C, A382T, N390D, N390S, and S393L) found in single sporadic ALS cases [14–21], most are located in the C-terminal Gly-rich region.

The C-terminal Gly-rich region of TDP-43 regulates the alternative splicing of several genes [22,23] and functions as a transcriptional repressor [24]. This domain also binds several heterogeneous nuclear ribonucleoproteins [2,25]. Furthermore, using a yeast TDP-43 proteinopathy model, it was shown that the C-terminal Gly-rich region is required for TDP-43 aggregation and cellular toxicity in vivo [26]. Therefore, phosphorylation and/or mutation of amino acid residue(s) in the C-terminal Gly-rich region of TDP-43 may significantly affect cellular function.

Previously, we reported that recombinant TDP-43 hyperphosphorylated with CK1 showed similar electrophoretic mobility to abnormally phosphorylated TDP-43 observed in the brains of patients with FTLD-U and ALS, and we suggested that CK1 was involved in the abnormal phosphorylation of TDP-43 [7,8]. We prepared 39 antibodies to predicted phosphorylation sites in TDP-43 [7]. Twenty-three of these predicted sites were found to be actually phosphorylated in vitro by CK1. Furthermore, 10 antibodies against actual phosphorylated sites, pS91, pS379, pS389, pS395, pS403, pS404, p403/404, pS409, p410 and pS409/410, were found to label hyperphosphorylated recombinant TDP-43, not non-phosphorylated recombinant TDP-43 [7,8,unpublished data]. Therefore, the specificity of these antibodies was confirmed.

Antibodies raised against Ser 379, Ser 403/404 and Ser 409/410 sites in the C-terminal Gly-rich region labeled TDP-43 accumulations and/or inclusion bodies in brains of patients with FTLD-U and ALS; they also recognized abnormally phosphorylated TDP-43 in the Sarkosyl-insoluble fractions from FTLD-U and ALS brains, and labeled abnormal fibers of 15 nm diameter in inclusion bodies in the spinal cord of ALS patients [7,8]. Furthermore, these antibodies recognized high-molecular-weight smearing, abnormally phosphorylated TDP-43 with a molecular weight of 45 kDa, and C-terminal fragments with molecular weights of 18–28 kDa in Sarkosyl-insoluble fractions from FTLD-U and ALS brain [7,8]. Therefore, at least the Ser 379, Ser 403/404 and Ser 409/410 sites in the C-terminal Gly-rich region, which were identified as in vivo targets of CK1 phosphorylation, may be abnormally phosphorylated in

FTLD-U and ALS brains. Recently, rat monoclonal antibodies raised against phosphorylated Ser 409/410 gave similar results [27], supporting our previous findings. Thus, abnormal phosphorylation of the C-terminal Gly-rich region of TDP-43 is a consistent feature of pathologic inclusions in FTLD-U and ALS brains [7,8,27], and may play a significant role in the cytoplasmic accumulation and the formation of inclusion bodies, as in the cases of tauopathy and alpha-synucleinopathy [28,29].

In summary, our results suggest that multiple Ser residues in the C-terminal Gly-rich region of TDP-43 are major CK1 phosphorylation targets. Furthermore, phosphorylation of Ser 379, Ser 403/404 and Ser 409/410, which we observed previously in TDP-43 accumulated in FTLD-U and ALS brains [7], is also mediated by CK1, indicating that CK1 may be involved in pathological phosphorylation of TDP-43 in vivo. The data on phosphorylation sites of TDP-43 presented here should be useful for further studies on the mechanism of TDP-43 proteinopathy.

Acknowledgments

This research was supported by a Grant-in-Aid for Scientific Research on Priority Areas – Research on Pathomechanisms of Brain Disorder (to H.M., 20023038), Grants-in-Aid for Scientific Research (B) (to H.M., 18300117 and to F.K., 20300144), Grants-in-Aid for Scientific Research (C) (to T.N., 19590297 and to T.A., 19591024) from the Ministry of Education, Culture, Sports, Science and Technology of Japan, and grants from the Ministry of Health, Labor and Welfare of Japan (to M.H.).

References

[1] S.H. Ou, F. Wu, D. Harrich, L.F. Garcia-Martinez, R.B. Gaynor, Cloning and characterization of a novel cellular protein, TDP-43, that binds to human immunodeficiency virus type 1 TAR DNA sequence motifs, J. Virol. 69 (1995) 3584–3596.
[2] H.-Y. Wang, I.F. Wang, J. Bose, C.K.J. Shen, Structural diversity and functional implications of the eukaryotic TDP gene family, Genomics 83 (2004) 130–139.
[3] E. Buratti, T. Dork, E. Zuccato, F. Pagani, M. Romano, F.E. Baralle, Nuclear factor TDP-43 and SR proteins promote in vitro and in vivo CFTR exon 9 skipping, EMBO J. 20 (2001) 1774–1784.
[4] J.K. Bose, I.F. Wang, L. Hung, W.-Y. Tarn, C.K.J. Shen, TDP-43 overexpression enhances exon-7 inclusion during SMN Pre-mRNA splicing, J. Biol. Chem. 283 (2008) 28852–28859.
[5] M. Neumann, D.M. Sampathu, L.K. Kwong, A.C. Truax, M.C. Micsenyi, T.T. Chou, J. Bruce, T. Schuck, M. Grossman, C.M. Clark, L.F. McCluskey, B.L. Miller, E. Masliah, I.R. Mackenzie, H. Feldman, W. Feiden, H.A. Kretzschmar, J.Q. Trojanowski, V.M.Y. Lee, Ubiquitinated TDP-43 in frontotemporal lobar degeneration and amyotrophic lateral sclerosis, Science 314 (2006) 130–133.
[6] T. Arai, M. Hasegawa, H. Akiyama, K. Ikeda, T. Nonaka, H. Mori, D. Mann, K. Tsuchiya, M. Yoshida, Y. Hashizume, T. Oda, TDP-43 is a component of ubiquitin-positive tau-negative inclusions in frontotemporal lobar degeneration and amyotrophic lateral sclerosis, Biochem. Biophys. Res. Commun. 351 (2006) 602–611.
[7] M. Hasegawa, T. Arai, T. Nonaka, F. Kametani, M. Yoshida, Y. Hashizume, H.G. Beach, E. Buratti, F.E. Baralle, M. Morita, I. Nakano, A. Oda, K. Tsuchiya, H. Akiyama, Phosphorylated TDP-43 in frontotemporal lobar degeneration and amyotrophic lateral sclerosis, Ann. Neurol. 64 (2008) 60–70.
[8] Y. Inukai, T. Nonaka, T. Arai, M. Yoshida, Y. Hashizume, T.G. Beach, E. Buratti, F.E. Baralle, H. Akiyama, S. Hisanaga, M. Hasegawa, Abnormal phosphorylation of Ser409/410 of TDP-43 in FTLD-U and ALS, FEBS Lett. 582 (2008) 2899–2904.
[9] T. Nonaka, T. Arai, E. Buratti, F.E. Baralle, H. Akiyama, M. Hasegawa, Phosphorylated and ubiquitinated TDP-43 pathological inclusions in ALS and FTLD-U are recapitulated in SH-SY5Y cells, FEBS Lett. 583 (2009) 394–400.
[10] X. Zhang, J. Ye, O.N. Jensen, P. Roepstorff, Highly efficient phosphopeptide enrichment by calcium phosphate precipitation combined with subsequent IMAC enrichment, Mol. Cell. Proteomics 6 (2007) 2032–2042.
[11] J.V. Olsen, B. Blagoev, F. Gnad, B. Macek, C. Kumar, P. Mortensen, M. Mann, Global, in vivo and site-specific phosphorylation dynamics in signaling networks, Cell 127 (2006) 635–648.
[12] N. Blom, T. Sicheritz-Ponten, R. Gupta, S. Gammeltoft, S. Brunak, Prediction of post-translational glycosylation and phosphorylation of proteins from the amino acid sequence, Proteomics 4 (2004) 1633–1649.
[13] NetPhosK server. Available from: http://www.cbs.dtu.dk/services/NetPhosK/.
[14] M.A. Gitcho, R.H. Baloh, S. Chakraverty, K. Mayo, J.B. Norton, D. Levitch, K.J. Hatanpaa, C.L. White 3rd, E.H. Bigio, R. Caselli, M. Baker, M.T. Al-Lozi, J.C. Morris, A. Pestronk, R. Rademakers, A.M. Goate, N.J. Cairns, *TDP-43* A315T mutation in familial motor neuron disease, Ann. Neurol. 63 (2008) 535–538.
[15] J. Sreedharan, I.P. Blair, V.B. Tripathi, X. Hu, C. Vance, B. Rogelj, S. Ackerley, J.C. Durnall, K.L. Williams, E. Buratti, F. Baralle, J. de Belleroche, J.D. Mitchell, P.N. Leigh, A. Al-Chalabi, C.C. Miller, G. Nicholson, C.E. Shaw, TDP-43 mutations in familial and sporadic amyotrophic lateral sclerosis, Science 319 (2008) 1668–1672.
[16] E. Kabashi, P.N. Valdmanis, P. Dion, D. Spiegelman, B.J. McConkey, C.V. Velde, J.-P. Bouchard, L. Lacomblez, K. Pochigaeva, F. Salachas, P.-F. Pradat, W. Camu, V. Meininger, N. Dupre, G.A. Rouleau, TARDBP mutations in individuals with sporadic and familial amyotrophic lateral sclerosis, Nat. Genet. 40 (2008) 572–574.
[17] V.M. Van Deerlin, J.B. Leverenz, L.M. Bekris, T.D. Bird, W. Yuan, L.B. Elman, D. Clay, E.M. Wood, A.S. Chen-Plotkin, M. Martinez-Lage, E. Steinbart, L. McCluskey, M. Grossman, M. Neumann, I.L. Wu, W.-S. Yang, R. Kalb, D.R. Galasko, T.J. Montine, J.Q. Trojanowski, V.M.Y. Lee, G.D. Schellenberg, C.-E. Yu, TARDBP mutations in amyotrophic lateral sclerosis with TDP-43 neuropathology: a genetic and histopathological analysis, Lancet Neurol. 7 (2008) 409–416.
[18] A. Yokoseki, A. Shiga, C.-F. Tan, A. Tagawa, H. Kaneko, A. Koyama, H. Eguchi, A. Tsujino, T. Ikeuchi, A. Kakita, K. Okamoto, M. Nishizawa, H. Takahashi, O. Onodera, TDP-43 mutation in familial amyotrophic lateral sclerosis, Ann. Neurol. 63 (2008) 538–542.
[19] N.J. Rutherford, Y.-J. Zhang, M. Baker, J.M. Gass, N.A. Finch, Y.-F. Xu, H. Stewart, B.J. Kelley, K. Kuntz, R.J.P. Crook, J. Sreedharan, C. Vance, E. Sorenson, C. Lippa, E.H. Bigio, D.H. Geschwind, D.S. Knopman, H. Mitsumoto, R.C. Petersen, N.R. Cashman, M. Hutton, C.E. Shaw, K.B. Boylan, B. Boeve, N.R. Graff-Radford, Z.K. Wszolek, R.J. Caselli, D.W. Dickson, I.R. Mackenzie, L. Petrucelli, R. Rademakers, Novel mutations in TARDBP (TDP-43) in patients with familial amyotrophic lateral sclerosis, PLoS Genet. 4 (2008) e1000193.
[20] P. Kuhnlein, A.D. Sperfeld, B. Vanmassenhove, V. Van Deerlin, V.M. Lee, J.Q. Trojanowski, H.A. Kretzschmar, A.C. Ludolph, M. Neumann, Two German kindreds with familial amyotrophic lateral sclerosis due to TARDBP mutations, Arch. Neurol. 65 (2008) 1185–1189.
[21] L. Corrado, A. Ratti, C. Gellera, E. Buratti, B. Castellotti, Y. Carlomagno, N. Ticozzi, L. Mazzini, L. Testa, F. Taroni, F.E. Baralle, V. Silani, S.D. Alfonso, High frequency of *TARDBP* gene mutations in Italian patients with amyotrophic lateral sclerosis, Hum. Mutat., 2009, doi:10.1002/humu.20950.
[22] Y.M. Ayala, S. Pantano, A. D'Ambrogio, E. Buratti, A. Brindisi, C. Marchetti, M. Romano, F.E. Baralle, Human, *Drosophila*, and *C. elegans* TDP43: nucleic acid binding properties and splicing regulatory function, J. Mol. Biol. 348 (2005) 575–588.
[23] P.A. Mercado, Y.M. Ayala, M. Romano, E. Buratti, F.E. Baralle, Depletion of TDP 43 overrides the need for exonic and intronic splicing enhancers in the human apoA-II gene, Nucl. Acids Res. 33 (2005) 6000–6010.
[24] M.M. Abhyankar, C. Urekar, P.P. Reddi, A novel CpG-free vertebrate insulator silences the testis-specific SP-10 gene in somatic tissues: role for TDP-43 in insulator function, J. Biol. Chem. 282 (2007) 36143–36154.
[25] E. Buratti, A. Brindisi, M. Giombi, S. Tisminetzky, Y.M. Ayala, F.E. Baralle, TDP-43 binds heterogeneous nuclear ribonucleoprotein A/B through its C-terminal tail: an important region for the inhibition of cystic fibrosis transmembrane conductance regulator exon 9 splicing, J. Biol. Chem. 280 (2005) 37572–37584.
[26] B.S. Johnson, J.M. McCaffery, S. Lindquist, A.D. Gitler, A yeast TDP-43 proteinopathy model: exploring the molecular determinants of TDP-43 aggregation and cellular toxicity, Proc. Natl. Acad. Sci. USA 105 (2008) 6439–6444.
[27] M. Neumann, L.K. Kwong, E.B. Lee, E. Kremmer, A. Flatley, Y. Xu, M.S. Forman, D. Troost, H.A. Kretzschmar, J.Q. Trojanowski, V.M. Lee, Phosphorylation of S409/410 of TDP-43 is a consistent feature in all sporadic and familial forms of TDP-43 proteinopathies, Acta Neuropathol. 117 (2009) 137–149.
[28] M. Hasegawa, R. Jakes, R.A. Crowther, V.M.Y. Lee, Y. Ihara, M. Goedert, Characterization of mAb AP422, a novel phosphorylation-dependent monoclonal antibody against tau protein, FEBS Lett. 384 (1996) 25–30.
[29] H. Fujiwara, M. Hasegawa, N. Dohmae, A. Kawashima, E. Masliah, M.S. Goldberg, J. Shen, K. Takio, T. Iwatsubo, alpha-Synuclein is phosphorylated in synucleinopathy lesions, Nat. Cell Biol. 4 (2002) 160–164.

8014 *Biochemistry* **2009,** *48,* 8014–8022
DOI: 10.1021/bi900619j

BIOCHEMISTRY
including biophysical chemistry & molecular biology
Article

A Cellular Model To Monitor Proteasome Dysfunction by α-Synuclein†

Takashi Nonaka* and Masato Hasegawa*

Department of Molecular Neurobiology, Tokyo Institute of Psychiatry, Tokyo Metropolitan Organization for Medical Research, 2-1-8 Kamikitazawa, Setagaya-ku, Tokyo 156-8585.

Received April 9, 2009; Revised Manuscript Received June 16, 2009

ABSTRACT: Impairment of the ubiquitin-proteasome degradation system has recently been suggested to be related to the onset of neurodegenerative disorders such as Alzheimer's disease and Parkinson's disease. In this study, we investigated whether intracellular α-synuclein affects proteasome activity in SH-SY5Y cells. To monitor intracellular proteasome activity, we used a reporter consisting of a short peptide degron fused to the carboxyl-terminus of green fluorescent protein (GFP-CL1), which is known to be degraded by proteasome. The level of intact GFP-CL1 was dramatically increased by coexpression of GFP-CL1 and α-synuclein, as judged by confocal microscopic and immunoblot analyses. Expression of two pathogenic mutants of α-synuclein, A30P and A53T, and phosphomimetic S129D mutant increased the intensities of GFP more effectively than did wild-type α-synuclein. GFP fluorescence in cells transfected with Δ73-83 mutant or β-synuclein, which does not assemble into filaments *in vitro*, was not changed as compared with that in cells expressing GFP-CL1 alone. Thus, the ability of α-synuclein to inhibit proteasome activity is related to its propensity to assemble into filaments. Furthermore, we observed that some compounds inhibiting α-synuclein filament formation *in vitro* prevented the α-synuclein-mediated proteasome dysfunction in cells transfected with both GFP-CL1 and α-synuclein. The cellular model expressing both GFP-CL1 and α-synuclein may be a useful tool to screen compounds protecting neurons from α-synuclein-mediated proteasome dysfunction.

Parkinson's disease (PD) is one of the most common neurodegenerative disorders. It is characterized by loss of dopaminergic neurons in the substantia nigra and by intracellular inclusion bodies known as Lewy bodies and Lewy neuritis. α-Synuclein is a natively unfolded protein and is deposited in a hyperphosphorylated form as the major component of these filamentous inclusions (*1*–*3*). Genetic studies have revealed that missense mutations (A30P, E46K, and A53T) in the α-synuclein gene cause familial forms of PD and dementia with Lewy bodies (DLB) (*4*–*6*). It has also been reported that multiplications (duplication and triplication) of α-synuclein gene cause an inherited form of PD and DLB (*7*–*11*). Thus, an increased level of intracellular α-synuclein is thought to contribute to the onset of familial PD.

Intracellular and extracellular protein deposits may cause neuronal cell death and may signal onset of many neurodegenerative diseases. We have reported that phosphorylated α-synuclein is partially ubiquitinated in α-synucleinopathy brains (*12*). We also found that ubiquitination of α-synuclein occurs in cultured cells at sites identical to those of filamentous α-synuclein ubiquitinated *in vitro*, suggesting that ubiquitination may be a late event in the formation of Lewy bodies (*13*). A recent paper confirmed our findings and showed that monoubiquitination and multiubiquitination at Lys12, 21, and 23 are detectable on phosphorylated α-synuclein in α-synucleinopathy brains (*14*). These findings indicate that the ubiquitin-proteasome system (UPS) is targeted to abnormal α-synuclein in the brains of patients but that ubiquitinated α-synuclein cannot be degraded by the UPS, suggesting that the UPS may not be effective to clear the abnormal form of α-synuclein.

The UPS functions in cellular quality control by degrading misfolded, unassembled, or damaged proteins that might create toxic intracellular aggregates (*15*, *16*). As the proteasome efficiently degrades multiubiquitinated proteins, the presence of elevated levels of ubiquitin conjugates in intracellular deposits of aggregated proteins in most neurodegenerative diseases suggests a linkage between UPS dysfunction and pathogenesis. Functional relationships between α-synuclein and the UPS have been described (*17*–*19*). Synder et al. reported that aggregated and monomeric α-synuclein inhibit proteasomal function *in vitro* (*20*). Lindersson et al. also observed proteasomal inhibition by α-synuclein filaments and oligomers *in vitro* (*21*). In cultured cells, it remains controversial whether expression of α-synuclein affects intracellular proteasome activity. Martin-Clemente et al. reported that α-synuclein expression level does not significantly affect proteasome function in PC12 cells (*22*), while Fujita et al. reported that proteasome activity was significantly decreased in cells overexpressing wild-type α-synuclein (*23*). Stefanis et al. described that expression of A53T mutant, but not wild-type α-synuclein, inhibits proteasome activity in PC12 cells (*24*). It was also reported that cell-produced α-synuclein oligomers are targeted to and impair the 26S proteasome (*25*).

Recently, Bence et al. reported impairment of the ubiquitin-proteasome system by the expression of an exon 1 fragment of

†This work was supported by a Grant-in-Aid for Scientific Research on Priority Areas—Research on Pathomechanisms of Brain Disorders (to M.H., 20023038) and Grants-in-Aid for Scientific Research (B) (to M.H., 18300117) and (C) (to T.N., 19590297) from the Ministry of Education, Culture, Sports, Science and Technology of Japan.

*To whom correspondence should be addressed. Phone: +81-3-3304-5701. Fax: +81-3-3329-8035. E-mail: nonakat@prit.go.jp, masato@prit.go.jp.

 Published on Web 07/24/2009

huntingtin containing expanded polyglutamine homopolymer in cultured cells (*26*). They used a green fluorescent protein (GFP) reporter that is specifically degraded by the cellular proteasome. This fluorescent reporter system is also useful for facile detection of proteasome activity in *Caenorhabditis elegans* (*27*).

In this study, to investigate whether intracellular α-synuclein affects proteasome activity, we have established a more sensitive assay system to monitor proteasome activity in cells using the GFP reporter and demonstrated impairment of proteasome function by expression of α-synuclein in SH-SY5Y cells. We also found that two pathogenic mutations of α-synuclein (A30P and A53T) and S129D mutant, which mimics phosphorylation, inhibit proteasome activity more effectively than does wild-type α-synuclein, while Δ73-83 mutant and β-synuclein, which do not form fibrils *in vitro*, do not affect proteasome function. Furthermore, we used our cellular model to screen for compounds protecting cells from proteasome inhibition by α-synuclein and found that some polyphenols attenuate α-synuclein-induced proteasome impairment.

EXPERIMENTAL PROCEDURES

Construction of Plasmids. The GFP-CL1 plasmid was constructed by digestion of pEGFP-C1 (Clontech) with *Bgl*II and *Sal*I and ligation with hybridized oligonucleotides termed CL1s (5′-GATCCGCTTGTAAAAATTGGTTTTCTTCTTT-ATCTCATTTTGTTATTCATTTATAAG-3′) and CL1a (5′-TCGACTTATAAATGAATAACAAAATGAGATAAAGA-AGAAAACCAATTTTTACAAGCG-3′). The resulting construct, the GFP gene containing an oligonucleotide encoding ACKNWFSSLSHFVIHL, was confirmed by DNA sequencing and designated pEGFP-CL1.

Human α-synuclein, β-synuclein, tau 3R1N, and 4R1N cDNAs in pRK172 vector were kind gifts from Dr. M. Goedert. The open reading frames of α-synuclein, β-synuclein, tau 3R1N, and 4R1N were subcloned into the mammalian expression vector pcDNA3. To construct plasmids encoding α-synuclein mutants A30P, A53T, S129A, and S129D, we performed site-directed mutagenesis using a site-directed mutagenesis kit (Strategene). We constructed a deletion mutant (residues 73−83: Δ73-83) of α-synuclein using PCR with the forward primer (5′-GGAG-CAGGGAGCATTGCAGCA-3′) and the reverse primer (5′-CGTCACCACTGCTCCTCCAAC-3′) using pcDNA3-α-synuclein as a template. The amplified fragments were self-ligated, and the resulting plasmids designated pcDNA-α-synuclein Δ73-83. All constructs were verified by DNA sequencing.

Cell Culture and Plasmid Expression. SH-SY5Y cells were cultured in DMEM/F12 medium (Sigma) supplemented with 10% (v/v) fetal calf serum, Penicillin-Streptomycin-Glutamine (GIBCO), and MEM Non-Essential Amino Acids Solution (GIBCO). The cells were maintained at 37 °C in a humidified atmosphere of 5% (v/v) CO_2. Cells were grown to 50% confluence in six-well culture dishes for transient expression and then transfected with various expression plasmids using FuGENE6 (Roche) according to the manufacturer's instructions.

Confocal Immunofluorescence Microscopy. SH-SY5Y cells were grown on a coverslip (15 mm × 15 mm) and transfected with expression vector (total 1.3 μg, e.g., 1 μg of pcDNA3-α-synuclein plus 0.3 μg of pEGFP-CL1). After incubation for indicated times, transfected cells on the coverslips were fixed with 4% (w/v) paraformaldehyde in phosphate-buffered saline (PBS) for 30 min. The coverslips were then incubated in 50 mM NH_4Cl in PBS for 10 min, and cell permeabilization was performed with 0.2% (v/v) Triton X-100 in PBS for 10 min. The cells were blocked for 30 min in 5% (w/v) BSA in PBS, then incubated with anti-α-synuclein monoclonal antibody, Syn102 (*28*) (1:500 dilution) for 1 h at 37 °C, followed by TRITC-labeled goat anti-mouse IgG (Sigma, 1:500 dilution) as the secondary antibody for 1 h at 37 °C. They were washed again and further incubated with TO-PRO-3 (Molecular Probes, 1:3000 dilution in PBS) for 45 min at 37 °C to stain nuclear DNA and analyzed using a LSM5 Pascal confocal laser microscope (Zeiss).

Sequential Extraction of Proteins and Immunoblotting. SH-SY5Y cells were grown in a six-well plate and transiently transfected with expression plasmids (total 1.3 μg). After incubation for 48−72 h, cells were harvested and lysed in TS buffer [50 mM Tris-HCl buffer, pH 7.5, 0.15 M NaCl, 5 mM ethylenediaminetetraacetic acid, 5 mM ethylene glycol bis(β-aminoethyl ether)-*N*,*N*,*N*,*N*-tetraacetic acid, and protease inhibitor cocktail (Roche)]. The lysate was centrifuged at 290,000*g* for 20 min at 4 °C, and the supernatant recovered as the TS-soluble fraction. The TS-insoluble pellet was lysed in TS buffer containing 1% (v/v) Triton X-100 (TX) and centrifuged at 290,000*g* for 20 min at 4 °C. The supernatant was collected as the TX-soluble fraction. The TX-insoluble pellet was further lyzed in SDS-sample buffer and heated for 5 min. Protein concentration was estimated by using the BCA Protein Assay Kit (Pierce). Samples (20 μg) were separated by 13.5% (v/v) SDS−PAGE using the Tris-tricine buffer system and proteins were transferred onto polyvinylidene difluoride membrane (Millipore). The blots were then blocked with 3% (v/v) gelatin and incubated overnight with anti-GFP monoclonal antibody (MBL), anti-Syn102, anti-human tau monoclonal antibody (HT7, Thermo Scientific) or anti-α-tublin monoclonal antibody (Sigma) in 10% (v/v) calf serum at a dilution of 1:1,000−5,000 at room temperature. After washing, blots were incubated with horseradish peroxidase-labeled secondary antibody (Bio-Rad) at a dilution of 1:10,000 in 10% (v/v) calf serum for 1 h at room temperature or a biotin-labeled secondary antibody (Vector) for 2 h at room temperature. Signals were detected using the chemiluminescence reagent Immunostar (Wako) or the ABC staining kit (Vector).

Measurement of Proteasome Activity Using a Peptide Substrate. SH-SY5Y cells transfected with expression plasmids were cultured for 72 h or treated with 20 μM MG132 for 6 h. Cells were harvested and cytosolic fraction was prepared as follows. Cells were resuspended in 100 μL of phosphate-buffered saline (PBS) and disrupted by sonication. Insoluble material was removed by ultracentrifugation at 290,000*g* for 20 min at 4 °C. The supernatant was assayed for proteasome activity by using a fluorescent peptide substrate, benzyloxycarbonyl-Leu-Leu-Glu-7-amido-4-methylcoumarin (z-LLE-MCA, Peptide Institute, Inc.). Aliquots (10 μL) were mixed with 0.1 M Tris-HCl buffer, pH 7.5 and water in a total volume of 1 mL. After preincubation at 37 °C for 10 min, 10 μL of 10 mM peptide substrate was added and the mixture was incubated for 30 min. A solution of 2% (v/v) acetic acid (1 mL) was added to the reaction mixture, and 7-amino-4-methylcoumarin (AMC) release was measured fluorometrically (excitation wavelength of 365 nm; emission wavelength of 460 nm). Enzyme activity was described as arbitrary unit/mg protein.

Screening for Compounds Preventing Proteasome Inhibition by α-Synuclein in Cultured Cells. SH-SY5Y cells were grown in six-well plates or on coverslips and transfected with both α-synuclein (1 μg) and GFP-CL1 plasmids (0.3 μg).

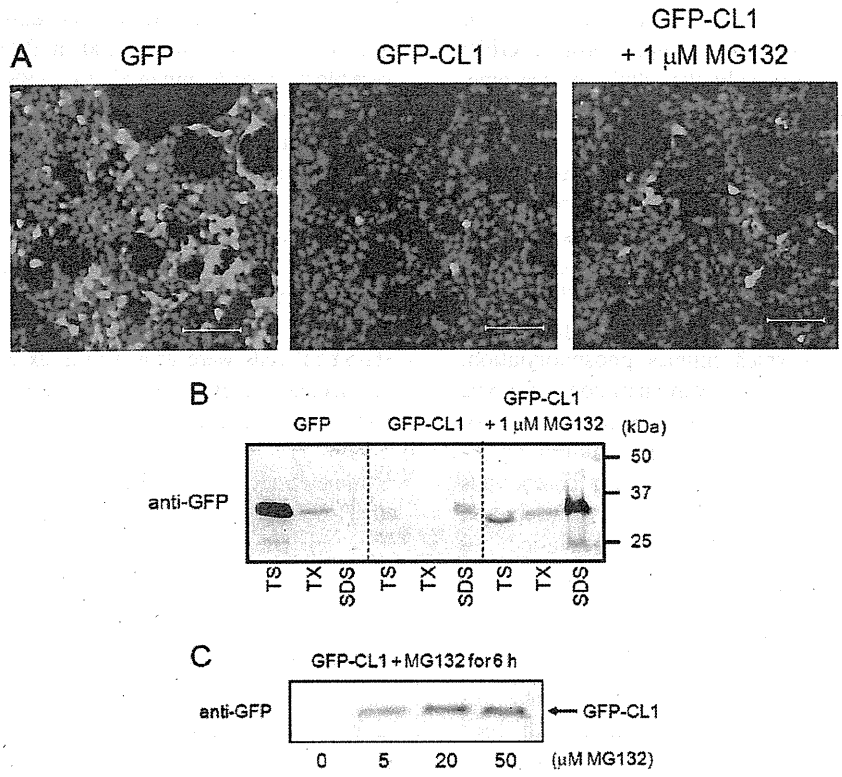

FIGURE 1: GFP-CL1 is degraded by proteasome in SH-SY5Y cells. (A) SH-SY5Y cells grown on coverslips were transfected with GFP or GFP-CL1 using FuGENE6. After an overnight incubation with or without 1 μM MG132, cells were fixed (total 48 h after transfestion), stained with TO-PRO-3 (Blue), and analyzed by confocal microscopy. Scale bar = 100 μm. (B) SH-SY5Y cells were transfected with GFP or GFP-CL1 and treated overnight with or without 1 μM MG132. Cells were harvested, and cell lysate was fractionated as described in Experimental Procedures and analyzed by immunoblotting using anti-GFP antibody. TS, Tris-soluble fraction; TX, Triton X-100-soluble fraction; SDS, SDS-soluble fraction. (C) SH-SY5Y cells were transfected with GFP-CL1 and treated with MG132 (0−50 μM) for 6 h. The cells were harvested, and the TX-insoluble fraction was analyzed by immunoblotting with anti-GFP antibody.

Various compounds (all at 40 μM) were added to the culture medium 2 h after transfection. Cells were harvested after incubation for 72 h, and the immunoblot and/or confocal microscopic analyses were performed as above. A decrease in GFP level in transfected cells treated with a compound, compared with the GFP level in transfected cells without such treatment, indicated that the compound rescues cells from proteasome dysfunction caused by expression of α-synuclein.

RESULTS

Cellular Expression of GFP-CL1. To establish a sensitive and convenient assay system for proteasome activity in cultured cells, we constructed GFP-CL1, which is GFP fused at the C-terminus with the 16-residue degron peptide CL1 (*26*, *29*). We transiently transfected SH-SY5Y cells with GFP or GFP-CL1, and analyzed the cells using confocal microscopy. As shown in Figure 1A, the fluorescence of GFP in cells transfected with GFP-CL1 was less than that in cells expressing GFP. The proteasome inhibitor MG132 increased fluorescence intensity in GFP-CL1-transfected cells (Figure 1A). Thus, we reconfirmed that the CL1 sequence specifically targeted normally stable GFP for efficient degradation by proteasome, as reported previously (*26*).

To biochemically characterize the proteasomal degradation of GFP-CL1, we fractionated lysates of cells transfected with GFP-CL1 or GFP. The TS-, TX-, and SDS-soluble fractions were analyzed by immunoblotting using anti-GFP antibody. As shown in Figure 1B, almost all GFP was recovered in the TS fraction in cells transfected with GFP, although a little GFP was detected in the TX-soluble fraction. In contrast, in cells expressing GFP-CL1, only weak GFP immunoreactivity was detected in the TS- and TX-insoluble fractions because of GFP-CL1 degradation by proteasome in transfected cells. Interestingly, in cells expressing GFP-CL1 treated with MG132, a band of uncleaved GFP-CL1 was detected in the SDS-soluble fraction in addition to the weak bands seen in the TS- and TX-soluble fractions, suggesting that uncleaved GFP-CL1 unexpectedly aggregates in cells when proteasome activity is inhibited by MG132 treatment. We also reconfirmed that MG132 treatment effectively and dose-dependently blocked the degradation of GFP-CL1 (Figure 1C).

Expression of α-Synuclein Inhibits Cellular Proteasome Activity. To investigate whether expression of α-synuclein might affect proteasome function in cultured cells, we cotransfected both α-synuclein and GFP-CL1 into SH-SY5Y cells. To reconfirm that GFP-CL1 is effectively degraded by proteasome, cells transfected with GFP-CL1 were treated with several protease inhibitors. SDS-soluble fraction of cell lysate was subjected to immunoblot analysis using anti-GFP antibody. As shown in Figure 2A, increased levels of GFP-CL1 band were observed in cells coexpressing GFP-CL1 and α-synuclein (lane 6), indicating that proteasome activity is inhibited effectively by expression of α-synuclein. Similar results were obtained when we treated cells expressing GFP-CL1 with MG132 or lactacystin (lane 3 and 4). On the other hand, leucyl-leucinal (LL, a calpain inhibitor) or chloroquine (a lysosomal inhibitor) did not inhibit GFP-CL1 degradation (lanes 2 and 5). We then tested whether the proteasome inhibition by α-synuclein is dose-dependent, i.e., dependent on the α-synuclein expression level. SH-SY5Y cells were

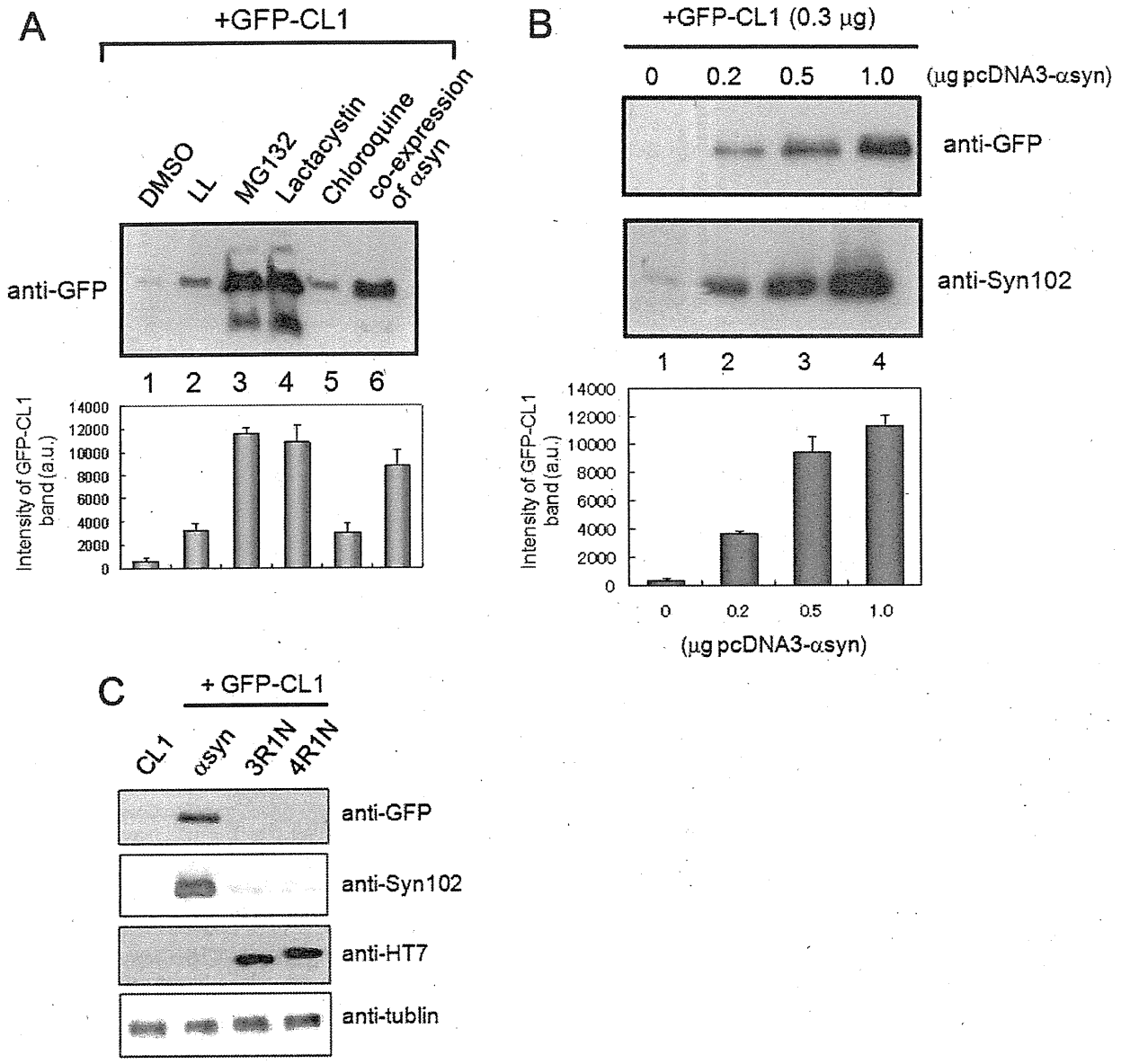

FIGURE 2: Expression of α-synuclein inhibits proteasome activity in SH-SY5Y cells. (A) SH-SY5Y cells transfected with GFP-CL1 were treated with 1 μM LL, MG132, lactacystin, and chloroquine overnight. In the case of coexpression, cells were transfected with both GFP-CL1 and α-synuclein using FuGENE6. The cells were harvested, and the Triton X-100-insoluble and SDS-soluble fractions were prepared and analyzed by immunoblotting using an anti-GFP antibody. The results of quantitative analysis of the GFP-CL1 bands, expressed as means + SD (n = 3), are shown below the blot. (B) SH-SY5Y cells were transfected with GFP-CL1 (0.3 μg), α-synuclein (0, 0.2, 0.5, or 1 μg), and/or pcDNA3 empty vector (total plasmids = 1.3 μg) and incubated for 72 h. The cells were harvested, and then Tris-soluble (lower panels) and SDS-soluble fractions (upper panels) were prepared. Immunoblot analyses were performed using anti-GFP (upper panels) or anti-Syn102 (lower panels) antibodies. The results of quantitative analysis of the GFP-CL1 bands, expressed as means + SD (n = 3), are shown below the blot. (C) SH-SY5Y cells were transfected with both GFP-CL1 (0.3 μg) and α-synuclein (1 μg) or pcDNA3-tau 3R1N or 4R1N vector (1 μg) and incubated for 72 h. The cells were harvested, and the TX-insoluble fraction was analyzed by immunoblotting with anti-GFP antibody. The TS-soluble fraction was also analyzed by using anti-Syn102, anti-HT7, and anti-tubulin antibodies (as a loading control).

transfected with both pEGFP-CL1 (0.3 μg) and pcDNA3-α-synuclein (0, 0.2, 0.5, or 1 μg; total 1.3 μg plasmids), followed by immunoblot analysis. The result showed that the level of intact GFP-CL1 increased in parallel with increased expression of α-synuclein (Figure 2B). Furthermore, we tested whether expression of tau protein which is also an effective substrate for proteasome (*30*), inhibits intracellular proteasome activity in SH-SY5Y cells. We found that expression of tau protein (3R1N and 4R1N) did not affect the proteasome activity in SH-SY5Y cells, suggesting that the effect of α-synuclein on the proteasome activity observed in this study is not simply due to overexpression of a protein, but is specific for α-synuclein. We also confirmed the absence of significant cell death in our cellular model transiently expressing α-synuclein, suggesting that the decreased proteasome activity found in cells expressing α-synuclein is not caused by cellular damage due to the toxicity of expressed α-synuclein.

To visually monitor proteasome inhibition due to expression of α-synuclein, SH-SY5Y cells were transiently cotransfected with α-synuclein and GFP-CL1, and transfected cells were analyzed by confocal microscopy. As shown in Figure 3C, the numbers of GFP-positive cells were significantly increased in cells transfected with wild-type α-synuclein and GFP-CL1, compared with cells transfected with GFP-CL1 alone (Figure 3B). This is in good agreement with the above immunoblotting data (Figure 2), indicating that expression of α-synuclein inhibited proteasome activity.

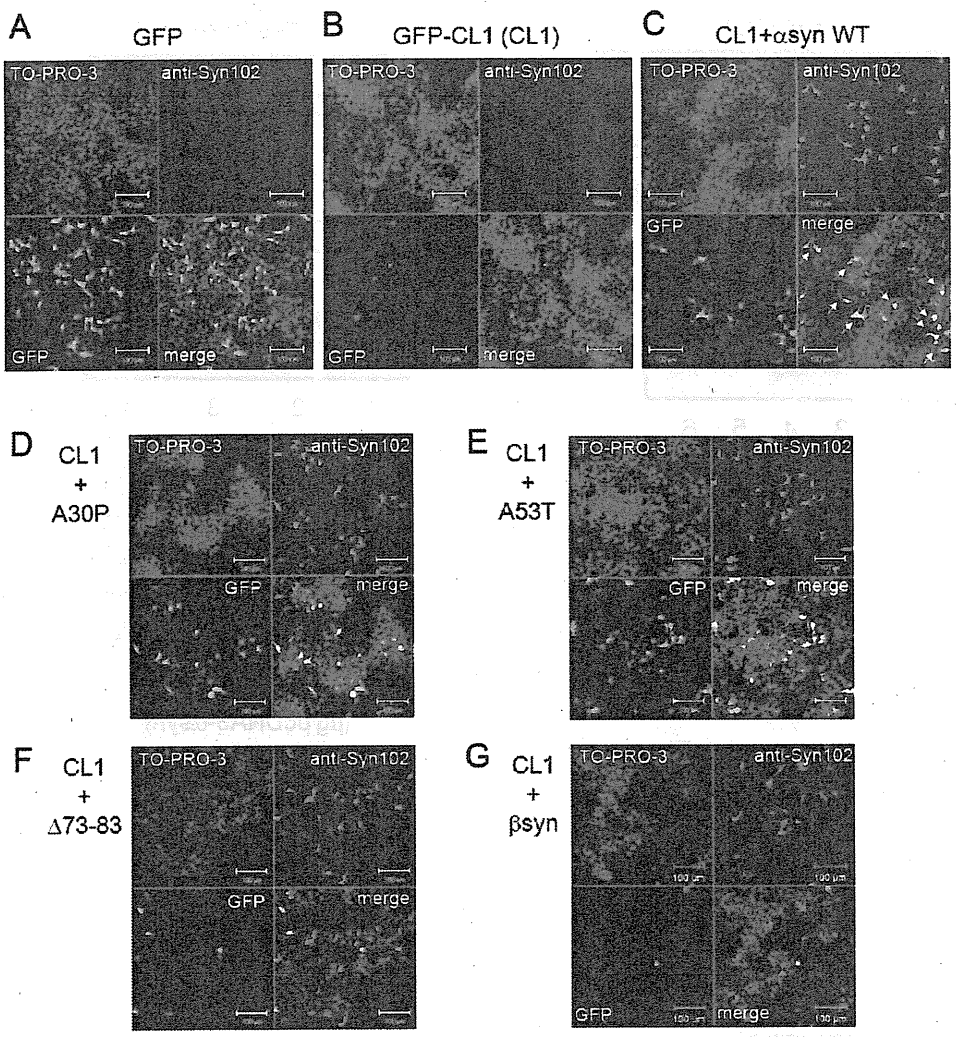

FIGURE 3: Expression of α-synuclein mutants affects proteasome activity in SH-SY5Y cells. SH-SY5Y cells grown on coverslips were transfected with GFP (A), GFP-CL1 (B), or both GFP-CL1 and wild-type α-synuclein (C), A30P (D), A53T (E), Δ73-83 (F), or β-synuclein (G). Cells were fixed 72 h after transfection and stained with anti-Syn102 (Red) and TO-PRO-3 (blue). Intracellular α-synuclein inhibits proteasome activity in cells expressing both GFP-CL1 and α-synuclein (arrows). Scale bar = 100 μm.

Taken together, these results showed that proteasome activity can be specifically and sensitively analyzed by monitoring the fluorescence intensity or immunoreactivity of GFP-CL1 in cultured cells and that the expression of α-synuclein impairs cellular proteasome function.

Effects of Expression of α-Synuclein Mutants and β-Synuclein on Proteasome Activity. Recombinant α-synuclein with a pathogenic mutation (A30P, A53T, or E46K) is more prone to assemble into filaments *in vitro* than the wild-type protein (*31*, *32*)). β-Synuclein and γ-synuclein (*33*) and the α-synuclein deletion mutant Δ73-83 (deletion of 73−83 residues) did not form fibrils *in vitro* (Nonaka et al., unpublished data). To study the effects of α-synuclein mutations on cellular proteasome activity, we transiently cotransfected these mutants and GFP-CL1 into SH-SY5Y cells and examined the cells using confocal microscopy. As shown in Figure 3, we found that increased GFP signals were observed in cells transfected with A30P (Figure 3D) or A53T (Figure 3E) compared with the signal seen in cells transfected with wild-type α-synuclein (Figure 3C), although the expression levels of the α-synuclein proteins were almost equal (Figure 3 and 4A). In contrast, little GFP fluorescence was detected in cells transfected with the α-synuclein deletion mutant Δ73-83 (Figure 3F) or β-synuclein (Figure 3G).

We also quantitatively examined the effects of these α-synuclein mutations on proteasome activity using immunoblot analysis. SH-SY5Y cells were transfected with both GFP-CL1 and wild-type α-synuclein, or the A30P, A53T, or Δ73-83 mutant, or β-synuclein. Uncleaved GFP-CL1 was recovered in the TX-insoluble (SDS-soluble) fraction as described above. As shown in Figure 4A, the level of uncleaved GFP-CL1 in cells transfected with A53T was about 30% higher than that in cells transfected with wild-type α-synuclein (Figure 4A, lane 4). A slightly higher level of GFP-CL1 was detected in cells transfected with the A30P mutant (Figure 4A, lane 3) compared with that in cells transfected with wild-type α-synuclein (Figure 4A, lane 2). In contrast, the level of GFP-CL1 in cells transfected with Δ73-83 or β-synuclein was negligible, as was that in control cells (Figure 4A, lane 5 and 6). The expression levels of α-synuclein protein in Tris-soluble fractions were almost the same. These results showed that mutants of α-synuclein that are prone to aggregate *in vitro* have stronger inhibitory effects on cellular proteasome activity than does the wild-type protein and that Δ73-83 and β-synuclein, neither of which form fibrils *in vitro*, do not inhibit the proteasome.

Expression of Phosphomimetic α-Synuclein Mutant S129D Enhanced Its Inhibition of Proteasome Activity. Aggregated α-synuclein in brains of α-synucleinopathy patients

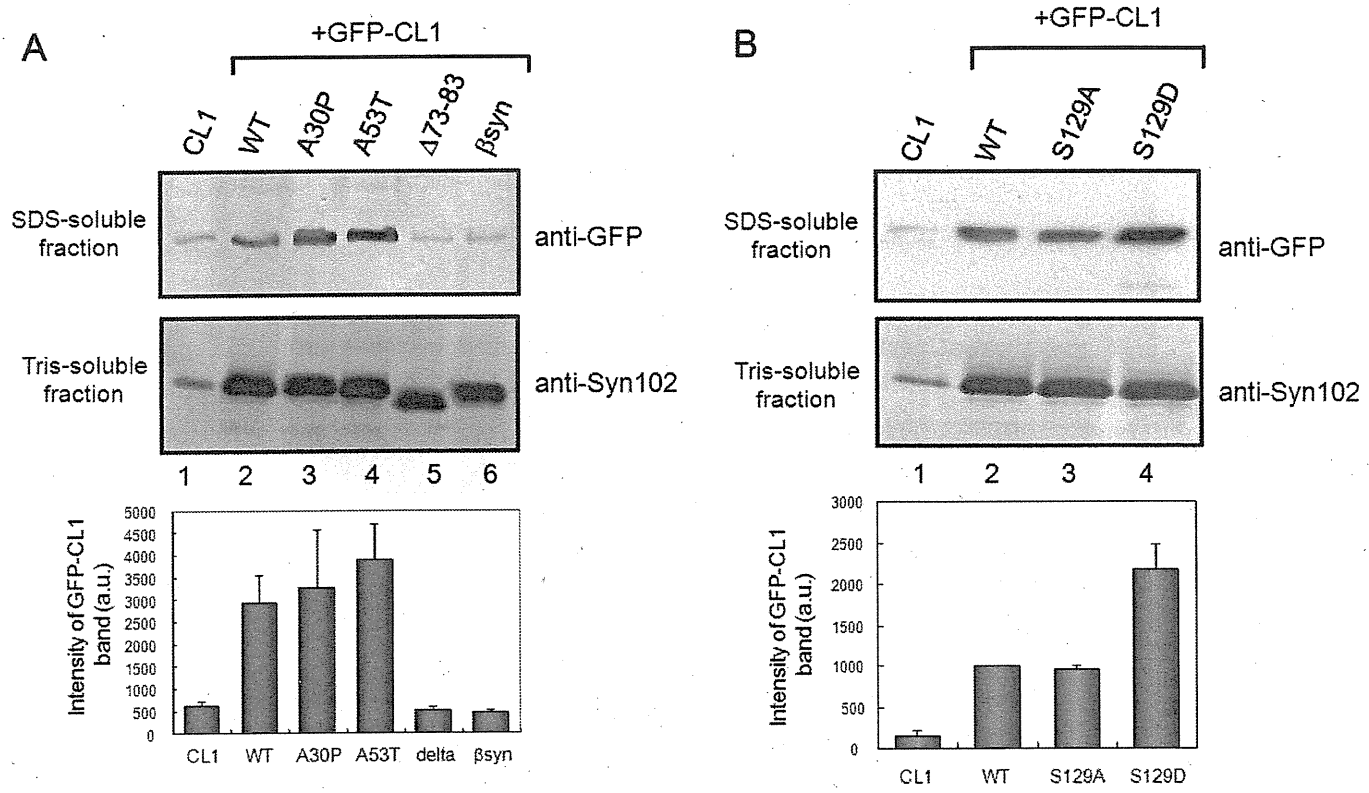

FIGURE 4: Effects of expression of α-synuclein mutants on proteasome activity. (A, B) Immunoblot analyses of extracted proteins from cells transfected with both GFP-CL1 and wild-type α-synuclein or a mutant (A30P, A53T, S129A, S129D, Δ73-83 or β-synuclein). Cells were harvested 72 h after transfection, and Tris-soluble (lower panels) and SDS-soluble fractions (upper panels) were prepared. Immunoblot analyses were performed using anti-GFP (upper panels) or anti-Syn102 (lower panels) antibodies. The results of quantitative analysis of the GFP-CL1 bands, expressed as means + SD (n = 3), are shown below the blot.

is hyperphosphorylated at Ser129, and this post-translational modification facilitates self-aggregation *in vitro* (*3*). Altering Ser129 to the negatively charged residue Asp (S129D) to mimic phosphorylation significantly enhances α-synuclein toxicity in a *Drosophila* model (*34*). We asked whether phosphorylation of α-synuclein might affect proteasome activity in cultured cells. SH-SY5Y cells were transfected with GFP-CL1 and wild-type or mutant α-synuclein. Immunoreactivity of GFP-CL1 in cells transfected with S129A was similar to that of cells transfected with wild-type α-synuclein, while the levels of GFP-CL1 in cells expressing S129D mutant to mimic phosphorylation was significantly higher than those in cells transfected with the wild-type or S129A (Figure 4B). These results suggested that phosphorylation of Ser129 may facilitate inhibition of proteasome function by intracellular α-synuclein.

Comparison of Proteasome Activity Assay Using GFP-CL1 with a Conventional Cleaving Assay Using a Fluorescent Peptide Substrate. To compare the sensitivity of the assay of proteasome activity using GFP-CL1 with that of the conventional assay using a fluorescent peptide, we evaluated biochemically the proteasome activity of lysates from cells transfected with α-synuclein. SH-SY5Y cells were transfected with wild-type α-synuclein for 72 h, and proteasome activity in cell lysates was measured using a peptide substrate specific for proteasome, zLLE-MCA. As shown in Figure 5, zLLE-MCA-cleaving activity in cells transfected with wild-type α-synuclein was decreased slightly (~10% inhibition) compared with that in cells transfected with empty vector, while MG132 had a potent inhibitory effect on proteasome activity (~80% inhibition). On the other hand, as described above, the levels of GFP-CL1 in cells transfected with GFP-CL1 and α-synuclein were increased about

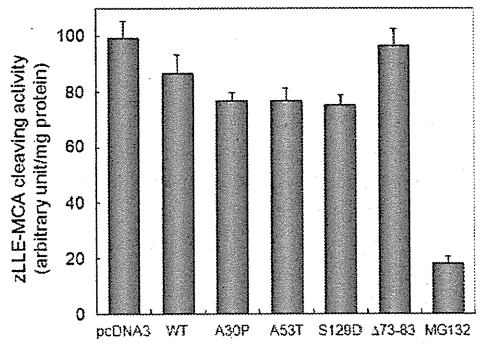

FIGURE 5: Measurements of proteasome activity using a fluorescent peptide substrate. SH-SY5Y cells were transfected with pcDNA3 empty vector, wild-type α-synuclein (WT), A30P, A53T, S129D, Δ73-83 for 72 h or treated with 20 μM MG132 for 6 h. Cytosolic fractions were prepared and assayed using z-LLE-MCA as a substrate. The results were expressed as means + SD (n = 3).

5 times compared with those in cells expressing GFP-CL1 (Figure 4A).

As shown in Figure 5, the zLLE-MCA-cleaving activity in cells transfected with A30P was almost equal to that in cells expressing A53T, which in turn was decreased slightly compared with that in cells transfected with wild-type α-synuclein. Proteasome activity in cells transfected with Δ73-83 was found to be the same as that in cells transfected with empty vector. It was also revealed that S129D had a slightly stronger inhibitory effect on proteasome activity than did wild-type α-synuclein. Taken together, as compared with the results shown in Figure 3 and 4, these results clearly indicate that a method in this study by detecting the fluorescence of GFP-CL1 or immunoblot analysis using

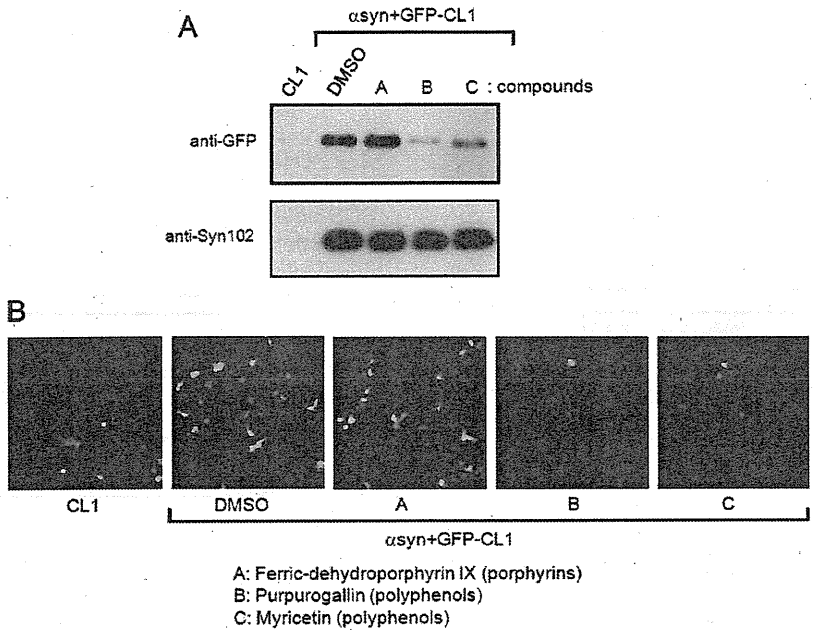

FIGURE 6: Small molecules prevent proteasome dysfunction by intracellular α-synuclein. SH-SY5Y cells were transfected with GFP-CL1 alone or both GFP-CL1 and α-synuclein. Compounds (final 40 μM) were added 2 h after transfection. Cells were harvested after a 72-h incubation and analyzed by immunoblotting (A) and confocal microscopy (B). Immunoblot analyses of Tris-soluble (lower panels) and SDS-soluble fractions (upper panels) were performed using anti-GFP (upper panels) or anti-Syn102 (lower panels) antibodies. The decreased GFP-CL1 level in transfected cells treated with compound B or C, as compared with that of transfected cells treated with vehicle alone (DMSO), indicated that compound B or C, but not compound A, rescued cells from proteasome impairment by expression of α-synuclein.

anti-GFP antibody is a simple and sensitive for monitoring proteasome activity in cells.

Small Molecular Compounds Attenuate Cellular Inhibition of Proteasome Activity by Expression of α-Synuclein. In this study, we have shown that proteasomal activity is impaired by expression of α-synuclein in SH-SY5Y cells. Impairment of proteasome function leads to induction of apoptosis, followed by cell death, so it is important to protect cells from such inhibition by intracellular α-synuclein. These results raised the possibility that our cellular model, in which both GFP-CL1 and α-synuclein are expressed, might be useful to screen for small molecules preventing proteasome inhibition mediated by expression of α-synuclein. Recently, we have reported that several compounds, including polyphenols, phenothiazines, and porphyrins, inhibit aggregation of recombinant α-synuclein *in vitro* (*35*). We therefore asked whether these compounds might affect proteasome inhibition by α-synuclein in cultured cells. Compounds of interest were added to the culture medium of cells transfected with both GFP-CL1 and α-synuclein 2 h after transfection. The cells were incubated for 72 h, harvested and analyzed by immunoblotting and confocal laser microscopy. Immunoblot analyses showed that the level of GFP-CL1 was decreased significantly when cells were treated with purpurogallin or myricetin (polyphenols), but not when they were treated with ferric-dehydroporphyrin IX (porphyrin) (Figure 6A). Cells treated with purpurogallin or myricetin displayed significant decreases in GFP-CL1 fluorescence by confocal microscopy (Figure 6B). Furthermore, we confirmed that exifone and gossypetin, plant polyphenols inhibiting fibril formation of α-synuclein *in vitro* (*35*), also attenuated α-synuclein-mediated proteasome inhibition (data not shown). We further observed that these small molecules did not affect α-synuclein expression (Figure 6A). These results indicate that these compounds may protect cells from proteasome dysfunction arising from expression of α-synuclein.

DISCUSSION

Recent studies have shown that aggregated and monomeric α-synuclein inhibit proteasomal function *in vitro* (*20*, *21*, *36*). In these reports, proteasome activity was measured in a cell-free system using fluorescent peptide substrates, and little is known about the effects of α-synuclein expression on proteasome activity in cultured cells. To examine this question, we tried to establish a sensitive and convenient method to measure proteasome activity using cultured cells transfected with a GFP-CL1 reporter plasmid. We further applied this system to show that transient coexpression of α-synuclein inhibits the proteasome activity of SH-SY5Y cells.

The GFP-CL1 reporter is a useful tool for the detection of proteasome activity in cells (*26*). Recently, Link et al. reported that the expression of GFP-CL1 in *Caenorhabditis elegans* muscle or neurons causes deposition of GFP-CL1 and leads to rapid paralysis (*27*). In this study, we also found that uncleaved GFP-CL1 was largely recovered in TX-insoluble fractions of SH-SY5Y cells transfected with GFP-CL1 and α-synuclein, while α-synuclein was recovered in TS- and TX-soluble fractions (Figure 1B and Figure S1 in Supporting Information), indicating that uncleaved GFP-CL1 was deposited, but α-synuclein was still soluble in transfected cells. Cell death was not detected in either cells transfected with GFP-CL1 alone or cells transfected with both GFP-CL1 and wild-type α-synuclein or mutants thereof, although Link et al. found that GFP-CL1 is toxic when expressed in *C. elegans* muscle cells (*27*). The discrepancy might be due to differences in the cell type used. Further studies are required in this regard. It is surprising that a relatively short addition of 16 residues to the C terminus of GFP can convert this normally soluble protein into a protein that strongly aggregates. We suggest that the C-terminal 16 residues may directly interfere with GFP folding, resulting in misfolded (but still fluorescent) forms that are prone to aggregate.

How does α-synuclein suppress intracellular proteasome activity? Several reports have described that α-synuclein may directly interfere with the proteasome. It was shown that α-synuclein binds to S6′ or S6a, a component of the 19S subunit in the 26S proteasome in cultured cells (*23*, *37*). It was also reported that aggregated α-synuclein, but not its monomer, effectively inhibited the 26S proteasome activity *in vitro* (*20*, *21*, *25*, *36*). Interestingly, we have shown that two pathogenic α-synuclein mutants, A30P and A53T, which are liable to form fibrils or oligomers *in vitro*, inhibited proteasome activity more strongly than did wild-type α-synuclein, while Δ73-83 mutant and β-synuclein, neither of which assemble into filaments *in vitro*, did not inhibit proteasome activity. Although we failed to detect any sarkosyl-insoluble aggregates of α-synuclein in cells transfected with wild-type or mutant α-synuclein (data not shown), these results raise the possibility that soluble prefibrillar intermediates, such as misfolded monomers, oligomers or protofibrils, may inhibit proteasome activity in transfected cells. Additional studies are needed to explore oligomers and protofibrils of α-synuclein in our cell model.

Phosphorylation seems to be a common mechanism controlling the neurotoxicity of aggregation-prone toxic proteins involved in neurodegenerative diseases such as tau (*38*, *39*), α-synuclein (*3*), and TDP-43 (*40*–*42*). We suggested that phosphorylation of α-synuclein may play a role in suppression of proteasome activity in cells. It was reported that expression of S129D mutant α-synuclein in *Drosophila* significantly enhances the toxicity (*34*). However, the mechanisms through which phosphomimetic S129D mutant causes cell death in the fly remain unknown. Phosphorylated α-synuclein at Ser129 is known to be more prone to aggregate than wild-type α-synuclein (*3*), and this may be related to its toxicity. Alternatively, inhibitory effects of the S129D mutant on intracellular proteasome activity, as shown in this study, may be involved in cell death.

Importantly, we have shown that intracellular α-synuclein may be toxic to neuronal cells because the protein causes proteasome dysfunction. It was previously reported that duplication and triplication of α-synuclein gene causes familial PD (*7*–*11*), indicating that overproduction of α-synuclein protein could lead to the onset of PD. It is reasonable to speculate that proteasome activity may also be affected in neurons of these patients in a manner similar to that shown in this study. It may be important to prevent α-synuclein-induced inhibition or decrease of proteasome activity. In this study, we screened for compounds protecting cells from the α-synuclein-mediated proteasome dysfunction and found that purpurogallin, myricetin, exifone, and gossypetin (polyphenols from plants) prevented proteasome impairment by α-synuclein. These compounds are thought to inhibit *in vitro* α-synuclein filament formation by stabilizing soluble prefibrillar intermediates (*35*). We speculate that these small molecules may interact with oligomeric forms of α-synuclein in cultured cells, although we can not exclude the possibility that these compounds directly regulate the activity of the proteasome. The precise mechanisms by which these polyphenols prevent α-synuclein-mediated proteasome dysfunction remain unknown. However, these compounds may be novel drug candidates for neurodegenerative diseases. Our cellular model system using coexpression of GFP-CL1 and α-synuclein should be a sensitive and useful tool for screening of compounds and drugs for the prevention and treatment of these disease.

ACKNOWLEDGMENT

We thank Drs. H. Mimuro and M. Masuda for helpful advice and discussions.

SUPPORTING INFORMATION AVAILABLE

Fractionation of cells expressing both of GFP-CL1 and α-synuclein. This material is available free of charge via the Internet at http://pubs.acs.org.

REFERENCES

1. Spillantini, M. G., Schmidt, M. L., Lee, V. M., Trojanowski, J. Q., Jakes, R., and Goedert, M. (1997) Alpha-synuclein in Lewy bodies. *Nature 388*, 839–840.
2. Baba, M., Nakajo, S., Tu, P. H., Tomita, T., Nakaya, K., Lee, V. M., Trojanowski, J. Q., and Iwatsubo, T. (1998) Aggregation of α-synuclein in Lewy bodies of sporadic Parkinson's disease and dementia with Lewy bodies. *Am. J. Pathol. 152*, 879–884.
3. Fujiwara, H., Hasegawa, M., Dohmae, N., Kawashima, A., Masliah, E., Goldberg, M. S., Shen, J., Takio, K., and Iwatsubo, T. (2002) α-Synuclein is phosphorylated in synucleinopathy lesions. *Nat. Cell Biol. 4*, 160–164.
4. Polymeropoulos, M. H., Lavedan, C., Leroy, E., Ide, S. E., Dehejia, A., Dutra, A., Pike, B., Root, H., Rubenstein, J., Boyer, R., Stenroos, E. S., Chandrasekharappa, S., Athanassiadou, A., Papapetropoulos, T., Johnson, W. G., Lazzarini, A. M., Duvoisin, R. C., Di Iorio, G., Golbe, L. I., and Nussbaum, R. L. (1997) Mutation in the α-synuclein gene identified in families with Parkinson's disease. *Science 276*, 2045–2047.
5. Kruger, R., Kuhn, W., Muller, T., Woitalla, D., Graeber, M., Kosel, S., Przuntek, H., Epplen, J. T., Schols, L., and Riess, O. (1998) Ala30Pro mutation in the gene encoding α-synuclein in Parkinson's disease. *Nat. Genet. 18*, 106–108.
6. Zarranz, J. J., Alegre, J., Gomez-Esteban, J. C., Lezcano, E., Ros, R., Ampuero, I., Vidal, L., Hoenicka, J., Rodriguez, O., Atares, B., Llorens, V., Gomez Tortosa, E., del Ser, T., Munoz, D. G., and de Yebenes, J. G. (2004) The new mutation, E46K, of α-synuclein causes Parkinson and Lewy body dementia. *Ann. Neurol. 55*, 164–173.
7. Singleton, A. B., Farrer, M., Johnson, J., Singleton, A., Hague, S., Kachergus, J., Hulihan, M., Peuralinna, T., Dutra, A., Nussbaum, R., Lincoln, S., Crawley, A., Hanson, M., Maraganore, D., Adler, C., Cookson, M. R., Muenter, M., Baptista, M., Miller, D., Blancato, J., Hardy, J., and Gwinn-Hardy, K. (2003) α-Synuclein locus triplication causes Parkinson's disease. *Science 302*, 841.
8. Chartier-Harlin, M. C., Kachergus, J., Roumier, C., Mouroux, V., Douay, X., Lincoln, S., Levecque, C., Larvor, L., Andrieux, J., Hulihan, M., Waucquier, N., Defebvre, L., Amouyel, P., Farrer, M., and Destee, A. (2004) Alpha-synuclein locus duplication as a cause of familial Parkinson's disease. *Lancet 364*, 1167–1169.
9. Ibanez, P., Bonnet, A. M., Debarges, B., Lohmann, E., Tison, F., Pollak, P., Agid, Y., Durr, A., and Brice, A. (2004) Causal relation between α-synuclein gene duplication and familial Parkinson's disease. *Lancet 364*, 1169–1171.
10. Nishioka, K., Hayashi, S., Farrer, M. J., Singleton, A. B., Yoshino, H., Imai, H., Kitami, T., Sato, K., Kuroda, R., Tomiyama, H., Mizoguchi, K., Murata, M., Toda, T., Imoto, I., Inazawa, J., Mizuno, Y., and Hattori, N. (2006) Clinical heterogeneity of α-synuclein gene duplication in Parkinson's disease. *Ann. Neurol. 59*, 298–309.
11. Ikeuchi, T., Kakita, A., Shiga, A., Kasuga, K., Kaneko, H., Tan, C. F., Idezuka, J., Wakabayashi, K., Onodera, O., Iwatsubo, T., Nishizawa, M., Takahashi, H., and Ishikawa, A. (2008) Patients homozygous and heterozygous for SNCA duplication in a family with parkinsonism and dementia. *Arch. Neurol. 65*, 514–519.
12. Hasegawa, M., Fujiwara, H., Nonaka, T., Wakabayashi, K., Takahashi, H., Lee, V. M., Trojanowski, J. Q., Mann, D., and Iwatsubo, T. (2002) Phosphorylated α-synuclein is ubiquitinated in α-synucleinopathy lesions. *J. Biol. Chem. 277*, 49071–49076.
13. Nonaka, T., Iwatsubo, T., and Hasegawa, M. (2005) Ubiquitination of α-synuclein. *Biochemistry 44*, 361–368.
14. Anderson, J. P., Walker, D. E., Goldstein, J. M., de Laat, R., Banducci, K., Caccavello, R. J., Barbour, R., Huang, J., Kling, K., Lee, M., Diep, L., Keim, P. S., Shen, X., Chataway, T., Schlossmacher, M. G., Seubert, P., Schenk, D., Sinha, S., Gai, W. P., and Chilcote, T. J. (2006) Phosphorylation of Ser-129 is the dominant pathological modification of α-synuclein in familial and sporadic Lewy body disease. *J. Biol. Chem. 281*, 29739–29752.

15. Ciechanover, A., Orian, A., and Schwartz, A. L. (2000) Ubiquitin-mediated proteolysis: biological regulation via destruction. *Bioessays 22*, 442–451.
16. Goldberg, A. L. (2003) Protein degradation and protection against misfolded or damaged proteins. *Nature 426*, 895–899.
17. Tofaris, G. K., Razzaq, A., Ghetti, B., Lilley, K. S., and Spillantini, M. G. (2003) Ubiquitination of α-synuclein in Lewy bodies is a pathological event not associated with impairment of proteasome function. *J. Biol. Chem. 278*, 44405–44411.
18. Sampathu, D. M., Giasson, B. I., Pawlyk, A. C., Trojanowski, J. Q., and Lee, V. M. (2003) Ubiquitination of α-synuclein is not required for formation of pathological inclusions in α-synucleinopathies. *Am. J. Pathol. 163*, 91–100.
19. Liu, C. W., Corboy, M. J., DeMartino, G. N., and Thomas, P. J. (2003) Endoproteolytic activity of the proteasome. *Science 299*, 408–411.
20. Snyder, H., Mensah, K., Theisler, C., Lee, J., Matouschek, A., and Wolozin, B. (2003) Aggregated and monomeric α-synuclein bind to the S6′ proteasomal protein and inhibit proteasomal function. *J. Biol. Chem. 278*, 11753–11759.
21. Lindersson, E., Beedholm, R., Hojrup, P., Moos, T., Gai, W., Hendil, K. B., and Jensen, P. H. (2004) Proteasomal inhibition by α-synuclein filaments and oligomers. *J. Biol. Chem. 279*, 12924–12934.
22. Martin-Clemente, B., Alvarez-Castelao, B., Mayo, I., Sierra, A. B., Diaz, V., Milan, M., Farinas, I., Gomez-Isla, T., Ferrer, I., and Castano, J. G. (2004) α-Synuclein expression levels do not significantly affect proteasome function and expression in mice and stably transfected PC12 cell lines. *J. Biol. Chem. 279*, 52984–52990.
23. Fujita, M., Sugama, S., Nakai, M., Takenouchi, T., Wei, J., Urano, T., Inoue, S., and Hashimoto, M. (2007) α-Synuclein stimulates differentiation of osteosarcoma cells: relevance to down-regulation of proteasome activity. *J. Biol. Chem. 282*, 5736–5748.
24. Stefanis, L., Larsen, K. E., Rideout, H. J., Sulzer, D., and Greene, L. A. (2001) Expression of A53T mutant but not wild-type α-synuclein in PC12 cells induces alterations of the ubiquitin-dependent degradation system, loss of dopamine release, and autophagic cell death. *J. Neurosci. 21*, 9549–9560.
25. Emmanouilidou, E., Stefanis, L., Vekrellis, K. (2008) Cell-produced α-synuclein oligomers are targeted to, and impair, the 26S proteasome, Neurobiol. Aging Epub ahead of print, DOI: 10.1016/j.neurobiolaging.2008.07.008.
26. Bence, N. F., Sampat, R. M., and Kopito, R. R. (2001) Impairment of the ubiquitin-proteasome system by protein aggregation. *Science 292*, 1552–1555.
27. Link, C. D., Fonte, V., Hiester, B., Yerg, J., Ferguson, J., Csontos, S., Silverman, M. A., and Stein, G. H. (2006) Conversion of green fluorescent protein into a toxic, aggregation-prone protein by C-terminal addition of a short peptide. *J. Biol. Chem. 281*, 1808–1816.
28. Tu, P. H., Galvin, J. E., Baba, M., Giasson, B., Tomita, T., Leight, S., Nakajo, S., Iwatsubo, T., Trojanowski, J. Q., and Lee, V. M. (1998) Glial cytoplasmic inclusions in white matter oligodendrocytes of multiple system atrophy brains contain insoluble α-synuclein. *Ann. Neurol. 44*, 415–422.
29. Gilon, T., Chomsky, O., and Kulka, R. G. (1998) Degradation signals for ubiquitin system proteolysis in *Saccharomyces cerevisiae*. *EMBO J. 17*, 2759–2766.
30. David, D. C., Layfield, R., Serpell, L., Narain, Y., Goedert, M., and Spillantini, M. G. (2002) Proteasomal degradation of tau protein. *J. Neurochem. 83*, 176–185.
31. Conway, K. A., Harper, J. D., and Lansbury, P. T. (1998) Accelerated *in vitro* fibril formation by a mutant α-synuclein linked to early-onset Parkinson disease. *Nat. Med. 4*, 1318–1320.
32. Choi, W., Zibaee, S., Jakes, R., Serpell, L. C., Davletov, B., Crowther, R. A., and Goedert, M. (2004) Mutation E46K increases phospholipid binding and assembly into filaments of human α-synuclein. *FEBS Lett. 576*, 363–368.
33. Biere, A. L., Wood, S. J., Wypych, J., Steavenson, S., Jiang, Y., Anafi, D., Jacobsen, F. W., Jarosinski, M. A., Wu, G. M., Louis, J. C., Martin, F., Narhi, L. O., and Citron, M. (2000) Parkinson's disease-associated α-synuclein is more fibrillogenic than β- and γ-synuclein and cannot cross-seed its homologs. *J. Biol. Chem. 275*, 34574–34579.
34. Chen, L., and Feany, M. B. (2005) α-Synuclein phosphorylation controls neurotoxicity and inclusion formation in a *Drosophila* model of Parkinson disease. *Nat. Neurosci. 8*, 657–663.
35. Masuda, M., Suzuki, N., Taniguchi, S., Oikawa, T., Nonaka, T., Iwatsubo, T., Hisanaga, S., Goedert, M., and Hasegawa, M. (2006) Small molecule inhibitors of α-synuclein filament assembly. *Biochemistry 45*, 6085–6094.
36. Snyder, H., Mensah, K., Hsu, C., Hashimoto, M., Surgucheva, I. G., Festoff, B., Surguchov, A., Masliah, E., Matouschek, A., and Wolozin, B. (2005) β-Synuclein reduces proteasomal inhibition by α-synuclein but not γ-synuclein. *J. Biol. Chem. 280*, 7562–7569.
37. Ghee, M., Fournier, A., and Mallet, J. (2000) Rat α-synuclein interacts with Tat binding protein 1, a component of the 26S proteasomal complex. *J Neurochem 75*, 2221–2224.
38. Morishima-Kawashima, M., Hasegawa, M., Takio, K., Suzuki, M., Yoshida, H., Titani, K., and Ihara, Y. (1995) Proline-directed and non-proline-directed phosphorylation of PHF-tau. *J. Biol. Chem. 270*, 823–829.
39. Hasegawa, M., Morishima-Kawashima, M., Takio, K., Suzuki, M., Titani, K., and Ihara, Y. (1992) Protein sequence and mass spectrometric analyses of tau in the Alzheimer's disease brain. *J. Biol. Chem. 267*, 17047–17054.
40. Nonaka, T., Arai, T., Buratti, E., Baralle, F. E., Akiyama, H., and Hasegawa, M. (2009) Phosphorylated and ubiquitinated TDP-43 pathological inclusions in ALS and FTLD-U are recapitulated in SH-SY5Y cells. *FEBS Lett. 583*, 394–400.
41. Inukai, Y., Nonaka, T., Arai, T., Yoshida, M., Hashizume, Y., Beach, T. G., Buratti, E., Baralle, F. E., Akiyama, H., Hisanaga, S., and Hasegawa, M. (2008) Abnormal phosphorylation of Ser409/410 of TDP-43 in FTLD-U and ALS. *FEBS Lett. 582*, 2899–2904.
42. Hasegawa, M., Arai, T., Nonaka, T., Kametani, F., Yoshida, M., Hashizume, Y., Beach, T. G., Buratti, E., Baralle, F., Morita, M., Nakano, I., Oda, T., Tsuchiya, K., and Akiyama, H. (2008) Phosphorylated TDP-43 in frontotemporal lobar degeneration and amyotrophic lateral sclerosis. *Ann. Neurol. 64*, 60–70.

FEBS Letters 583 (2009) 2419–2424

FEBS Letters

journal homepage: www.FEBSLetters.org

Methylene blue and dimebon inhibit aggregation of TDP-43 in cellular models

Makiko Yamashita [a,1], Takashi Nonaka [a,1], Tetsuaki Arai [b], Fuyuki Kametani [a], Vladimir L. Buchman [c], Natalia Ninkina [c,d], Sergey O. Bachurin [d], Haruhiko Akiyama [b], Michel Goedert [e], Masato Hasegawa [a,*]

[a] Department of Molecular Neurobiology, Tokyo Institute of Psychiatry, Tokyo Metropolitan Organization for Medical Reearch, 2-1-8 Kamikitazawa, Setagaya-ku, Tokyo 156-8585, Japan
[b] Department of Psychogeriatrics, Tokyo Institute of Psychiatry, Tokyo Metropolitan Organization for Medical Research, 2-1-8 Kamikitazawa, Setagaya-ku, Tokyo 156-8585, Japan
[c] School of Biosciences, Cardiff University, Cardiff CF10 3US, UK
[d] Institute of Physiologically Active Compounds, RAS, Chernogolovka 142432, Russian Federation
[e] MRC Laboratory of Molecular Biology, Hills Road, Cambridge CB2 0QH, UK

ARTICLE INFO

Article history:
Received 18 May 2009
Revised 10 June 2009
Accepted 22 June 2009
Available online 26 June 2009

Edited by Jesus Avila

Keywords:
Tau
Alpha-synuclein
Inhibitor
Alzheimer
ALS
FTLD

ABSTRACT

Amyotrophic lateral sclerosis (ALS) and frontotemporal lobar degeneration with ubiquitinated inclusions (FTLD-U) are major neurodegenerative diseases with TDP-43 pathology. Here we investigated the effects of methylene blue (MB) and dimebon, two compounds that have been reported to be beneficial in phase II clinical trials of Alzheimer's disease (AD), on the formation of TDP-43 aggregates in SH-SY5Y cells. Following treatment with 0.05 μM MB or 5 μM dimebon, the number of TDP-43 aggregates was reduced by 50% and 45%, respectively. The combined use of MB and dimebon resulted in a 80% reduction in the number. These findings were confirmed by immunoblot analysis. The results indicate that MB and dimebon may be useful for the treatment of ALS, FTLD-U and other TDP-43 proteinopathies.

1. Introduction

Amyotrophic lateral sclerosis (ALS) is a neurodegenerative disease that is characterized by progressive weakness and muscle wasting, and for which no effective therapies exist. Frontotemporal lobar degeneration (FTLD) is the second most common form of dementia after Alzheimer's disease (AD) in the population below the age of 65 years. In many cases with these disorders, ubiquitin (Ub)-positive, tau-negative intracytoplasmic inclusions form in nerve cells and glial cells. TAR DNA binding protein of 43 kDa (TDP-43) is the major component of these inclusions [1–3]. Biochemical and histological analyses demonstrated that TDP-43 accumulates in brain and spinal cord in a hyperphosphorylated and fibrillar form [4]. Furthermore, missense mutations in the TDP-43 gene have been identified in familial cases of ALS and ALS with FTLD-U [5–9]. Together, these findings indicate that dysfunction of TDP-43 is central to the etiology and pathogenesis of ALS and FTLD-U. In addition, TDP-43 has also been found to accumulate in other neurodegenerative disorders, including AD, dementia with Lewy bodies [10], Parkinsonism-dementia complex of Guam [11], argyrophilic grain disease [12], Huntington's disease [13], Perry syndrome [14] and familial British dementia [15].

Inhibition of the aggregation of TDP-43 and promotion of its clearance are considered to be major therapeutic avenues for ALS and FTLD-U. As for other neurodegenerative diseases, current tools include antibodies, synthetic peptides, molecular chaperones and chemical compounds. Of the latter, methylene blue (MB) and dimebon have recently been reported to have significant beneficial effects in phase II clinical trials of AD [16,17]. MB is a phenothiazine compound that has been used for treating methemoglobinemia [18,19], inhibiting nitric oxide synthase [20], reducing nGMP [21], enhancing β-oxydation in mitochondria [22], inhibiting of noradrenaline re-uptake [23] and enhancing brain mitochondrial cytochrome oxidase activity [24,25]. It has also been shown to inhibit AD-like Aβ and tau aggregation in vitro [26,27]. Dimebon is a non-selective anti-histaminergic compound that was in clinical use for many years before more selective agents became available [28]. It has been reported to inhibit butyrylcholinesterase, acetylcholinesterase, NMDA receptors, voltage-gated calcium channels, adrenergic receptors, histamine H1 receptors, histamine H2 receptors and serotonin receptors, as well as to stabilize glutamate-induced Ca^{2+} signals [29–31]. The effects of dimebon on pathological protein aggregation have not been studied in detail, but recently we demonstrated that chronic administration of this drug reduced

* Corresponding author. Fax: +81 3 3329 8035.
E-mail address: masato@prit.go.jp (M. Hasegawa).
[1] These authors contributed equally to this work.

0014-5793/$36.00
doi:10.1016/j.febslet.2009.06.042

the number of nerve cell deposits in a mouse model of synucleinopathy [32].

Here we investigated whether MB and dimebon can reduce the formation of TDP-43 inclusions in SH-SY5Y cellular models. Significantly, the treatment of cells with each compound and their combined application inhibited the formation of TDP-43 aggregates, suggesting that MB and dimebon may be effective for the treatment of ALS and FTLD-U.

2. Materials and methods

2.1. Antibodies

A polyclonal anti-TDP-43 antibody (anti-TDP-43) was purchased from ProteinTech Group Inc. (10782-1-AP, Chicago, USA). A polyclonal antibody specific for phosphorylated TDP-43 (anti-pS409/410) (available from Cosmo Bio Co., Tokyo, Japan) [4] and an anti-Ub antibody (MAB1510, Chemicon, Billerica, USA) were used for the evaluation of pathological forms of TDP-43.

2.2. TDP-43 cellular models and addition of compounds

To investigate the effects of MB and dimebon on the formation of TDP-43 aggregates, we used two cellular models of TDP-43 proteinopathy. The first consists of SH-SY5Y cells expressing mutant TDP-43 that lacks both the nuclear localization signal (NLS) and residues 187–192 (ΔNLS&187-192). In these cells, round structures positive for both anti-pS409/410 and anti-Ub are observed [33]. The second model consists of SH-SY5Y cells expressing an aggregation-prone TDP-43 C-terminal fragment (residues 162–

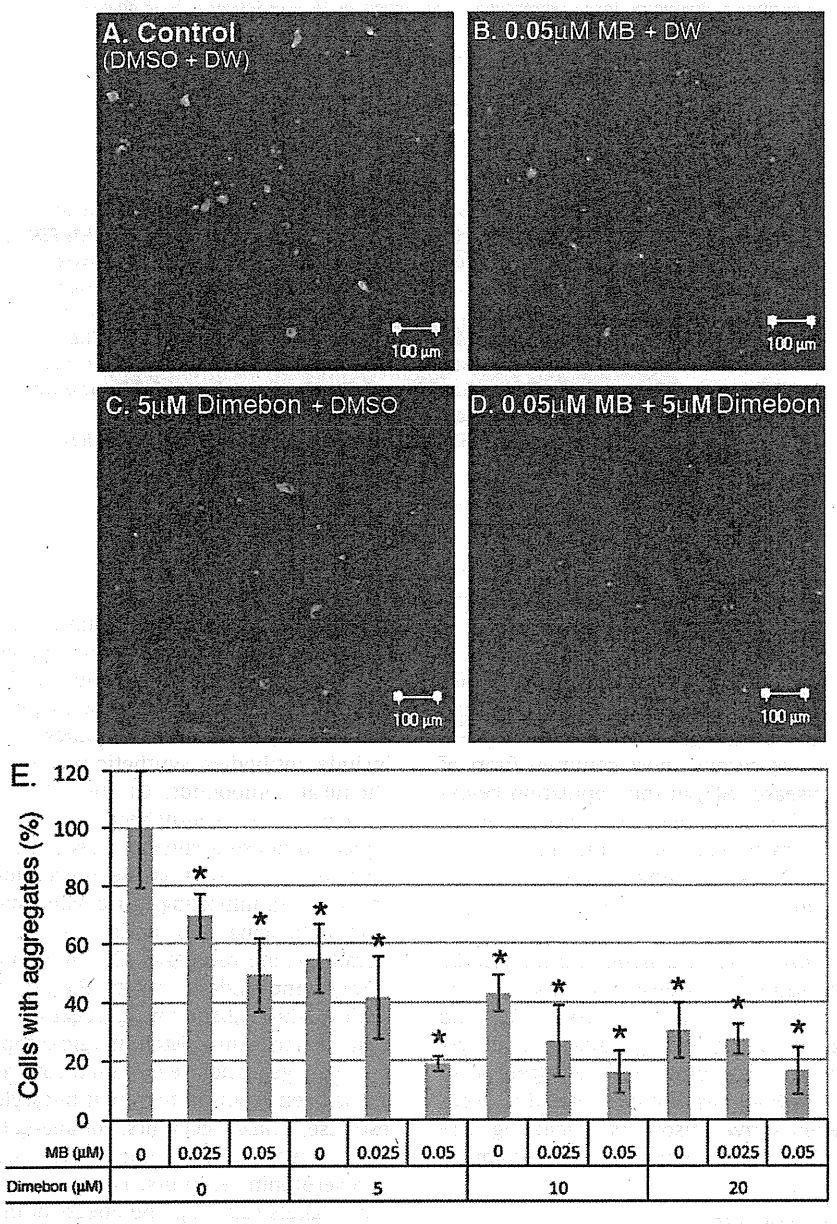

Fig. 1. Immunohistochemical analysis of the effects of methylene blue (MB) and dimebon on the aggregation of TDP-43 in SH-SY5Y cells expressing TDP-43 (ΔNLS&187-192). TDP-43 inclusions were stained with anti-pS409/410 antibody and detected with Alexa Fluor 488-labeled secondary antibody. Representative confocal images from cells treated with control (DMSO + DW) (A), 0.05 μM MB + DW (B), 5 μM dimebon + DMSO (C) and 0.05 μM MB + 5 μM dimebon (D) are shown. (E) Quantitation of cells with TDP-43 aggregates. The number of cells with intracellular TDP-43 aggregates was counted and expressed as the percentage of cells with aggregates in the absence of compound (taken as 100%). Fluorescence intensity within an area of approximately 800 μm × 800 μm was assessed by confocal microscopy. The intensity of Alexa Fluor 488 was calculated as the ratio of that of TO-PRO-3. At least 8 areas per sample were measured (n = 8–16). Data are means ± S.E.M. $^{*}P < 0.01$ by Student's t test.